# Anti-inflammation and adipogenesis inhibition functions of stylissatin A

(Stylissatin A の抗炎症および抗肥満活性に関する研究)

2020

筑波大学グローバル教育院
School of the Integrative and Global Majors in
University of Tsukuba
Ph.D. program in Human Biology

Zhang Menghua

筑波大学

University of Tsukuba

# 博士（人間生物学）学位論文

PhD dissertation in Human Biology

# Anti-inflammation and adipogenesis inhibition functions of stylissatin A

(Stylissatin A の抗炎症および抗肥満活性に関する研究)

2020

筑波大学グローバル教育院
School of the Integrative and Global Majors in
University of Tsukuba
Ph.D. program in Human Biology

Zhang Menghua

Table of contents

# **Chapter 1**. Abstract

The inflammatory response is a localized defense mechanism used by the body following a physical injury or infection. Pain, heat, and redness are the common clinical symptoms of inflammation. But at the same time, inflammation could also lead to severe diseases, such as hay fever, periodontitis and even cancer. It is obvious that inflammation is always with us human beings in our daily life.

Stylissatin A (SA), a cyclic peptide with anti-inflammation effect, was isolated from a marine sponge named *Stylissa massa*. Besides its anti-inflammation effect, what caught our interest is "cyclic peptide", which is the most characteristic feature of SA. Recently, cyclic peptides are gaining attention as candidates for "medium-size molecule drug discovery" because the conformation of cyclic peptides is restricted compared to linear compounds. They tend to strongly interact with specific target biomacromolecules and often develop stronger pharmacological activities. SA is a cyclic peptide composed of seven L-amino acids. Based on SAR study, D-Tyr$^1$-*t*BuSA, one of the synthetic derivatives of SA, was found to show most potent anti-inflammation function against LPS-stimulated murine (RAW264.7) macrophage cells (NO production inhibitory activity). What's more, it was also verified that D-Tyr$^1$-*t*BuSA showed potent anti-inflammation function by suppressing the expression of iNOS in a concentration-dependent manner. On the other hand, D-Tyr$^1$-*t*BuSA inhibited the differentiation of murine fibroblasts (3T3-L1) into adipocytes and lipid droplet accumulation. Western blot assay proved that D-Tyr$^1$-*t*BuSA showed adipogenesis inhibitory activity through the suppression of PPARγ and C/EPBα expression. In order to clarify the target proteins, SA biotin probe (SA-BP) was synthesized and used for affinity purification. Interestingly, a target protein ACADL (45 kDa, Acyl-CoA dehydrogenase, long chain), which catalyzes the β-oxidation of long chain acyl-CoA, was identified for both RAW264.7 and 3T3-L1 cells. Enzyme assay using FAD kit showed that

ACADL was inhibited by SA and D-Tyr$^1$-*t*BuSA, which means SA and its derivatives might specifically regulate intracellular signaling pathways that is common to inflammation and adipogenesis. Thus, a proposed mechanism was suggested. If the enzymatic activity of ACADL is inhibited by SA analogs, the amounts of liberated fatty acids would increase. In macrophage cells, increased fatty acids might activate PPARα, which triggers IκBα and results in the NF-κB inhibition. Thus, both the production of inflammatory cytokines IL-6 and TNF-α, and the expression level of iNOS are inhibited, as observed in RAW264.7 cells, which may count for anti-inflammatory activity. While, in 3T3-L1 cells, according to the proposed mechanism, increased fatty acids might activate PPARγ. However, this hypothesis did not match to the results of cellular expression levels of PPARγ treated with SA derivatives. In the proposed mechanism, activated PPARγ would induce cell differentiation of preadipocytes and result in fat accumulation. However, SA and its derivatives inhibited them and reduced triacylglycerol accumulation levels in mature adipocytes. Further elucidation of the mechanism of SA and its derivatives might establish new cellular targets and intracellular signaling pathways related to adipocyte differentiation and obesity.

Keywords: Cyclic peptide; Anti-inflammation activity; Adipogenesis inhibitory activity; Target molecules; Mode of action

# **Chapter 2**. Introduction

## 2-1 Natural Products Chemistry

Natural product chemistry is a branch of organic chemistry that deals with substances produced by living organisms. It is said that natural product chemistry has a long history which can date back to the late 18th century. In 1817, F. W. Sertürner (1783-1841) isolated a crystal of a highly anesthetic substance from opium and named it morphine[1]. With the discovery of this morphine, a number of natural products such as quinine and penicillin have been discovered, leading natural product chemistry to a new stage[2] (Figure 1).

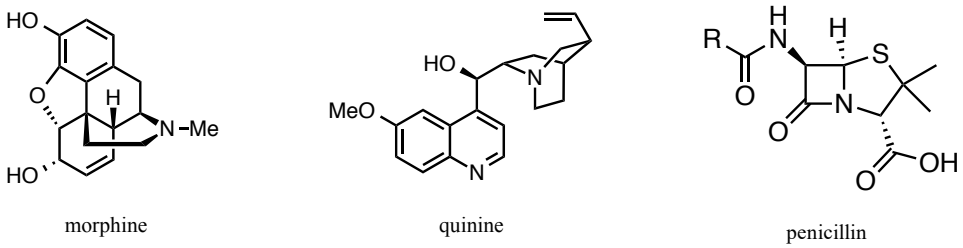


**Fig 1**. Natural organic compounds isolated in the 19th century

Natural product chemistry began with the extraction and separation of active ingredients from natural products. However, with the development of synthetic organic chemistry, total synthesis of natural products became a part of it. A well-known example was the isolation of salicin from willow trees in the 19th century. Salicin was used as an antipyretic analgesic until 1897, when Felix Hoffmann synthesized acetylsalicylic acid which later named as aspirin[3] (Figure 2). Since then, nature products became a big source of medicinal agents and natural product chemistry started to play a vital part in drug discovery research.

Following with the serendipitous discovery of penicillin from the filamentous fungus *Penicillium notatum* in 1929 and streptomycin by Selman A. Waksman in 1952, not only chemical synthesis, but

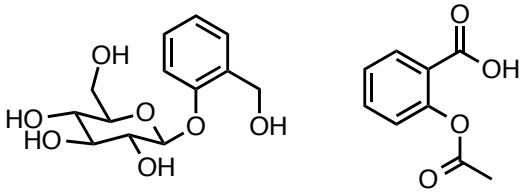


salicin

acetylsalicylic acid
(aspirin)

**Fig 2**. Natural products used as pharmaceuticals

also biosynthesis is included in the natural products chemistry[4,5] (Figure 3). Biological activity assays, elucidation of the mechanism of actions, and structure-activity relationships research also became a part of this research field with the development of science.

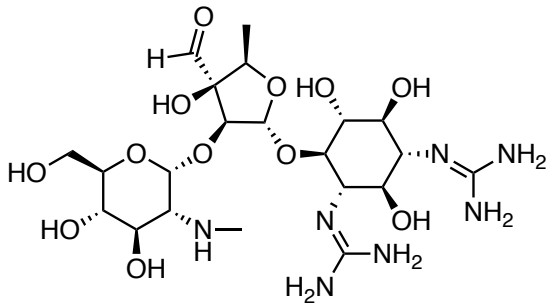


**Fig 3**. Structure of streptomycin

Nature creates wonderful substances out of human wisdom even in today's advanced science. The science of discovering such substances and studying them is still a trend.

## 2-2 Marine Natural Products

Nowadays, research interests in natural product chemistry have expanded to not only terrestrial animals, plants and microorganisms, but also marine organisms such as sea squirts and sponges. With the development of the new submersible "Aqualung" in 1943[6], which made scuba diving become popular, researchers became able to observe and collect marine life. Due to the unique environment of the ocean, many biologically active natural products with diverse and unique structures have been discovered.

The famous example is tetrodotoxin (TTX) (Figure 4). TTX was extracted from puffer fish and is well-known for its potent neurotoxic activity with $Na^+$ channel blocking action, discovered in the early 1960s[7]. TTX is very toxic to mammals with an $LD_{50}$ in the order of 10 mg/kg. In addition, many synthetic studies have been carried out due to the very unusual structure of the dioxa-adamantane skeleton, in which several polar functional groups are arranged. At first, it was generally thought that TTX was produced by puffer fish, however, TTX was also found in a completely different species of organism. Later, it became clear that TTX is produced by marine bacteria, proving the hypothesis that the food chain causes TTX to accumulate in organisms such as puffer fish. What's more, the potent channel blocking activity of TTX has greatly contributed to the study of the physiology of ion channels.

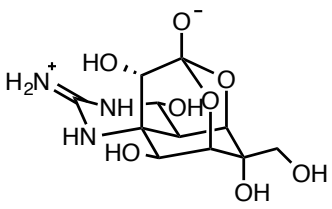


**Fig 4**. Structure of TTX

Another famous marine nature product is maitotoxin (MTX) (Figure 5). MTX is a unique

compound due to its molecular size and structural complexity, and shows extremely potent bioactivity, which activates $Ca^{2+}$ channel[8,9]. Except for macromolecules with repeating structures, such as proteins, nucleic acids, and polysacchalides, MTX is known as the largest natural products in molecular weight.

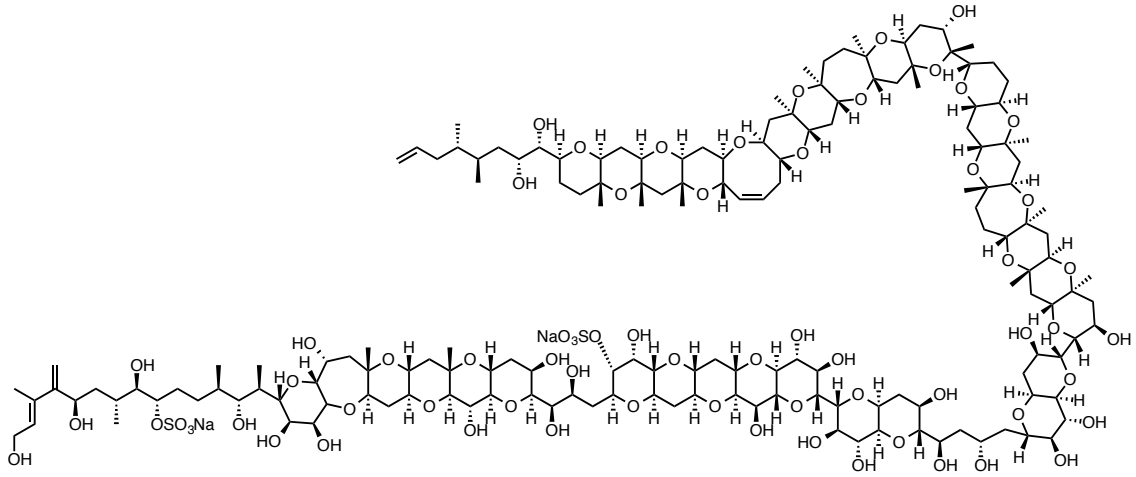

**Fig 5**. Structure of maitotoxin

Marine natural products with such diverse structures and biological activities have great potential as unique research tools in life sciences and on drug discovery.

## 2-3 Bioactive peptides and cyclic peptides

The diversity of organisms in the marine environment has inspired researchers to identify novel marine natural products that could eventually be developed into therapeutics. Many kinds of marine-derived pharmaceuticals have been discovered, including peptides. Peptides have a wide variety of lengths, shapes, amino acid sequences and post-translational modifications. Many bioactive peptides have been isolated so far, which later applied to research for pharmaceutical products, expressing various physiological functions and controlling many biological phenomena in living organisms. For example, in 1987, Pettit and his colleagues isolated a linear pentapeptide dolastatin 10 (Figure 6) from the sea slug *Dolabella auricularis*. This compound has strong cytotoxicity and antitumor activity, which has attracted attention as a promising lead compound for anticancer agents[10]. Among bioactive peptides, cyclic peptides have been particularly noticed in recent years. Cyclic peptides are expected to interact more strongly with specific target molecules than linear peptides because their conformations are restricted due to their macrocycle structures.

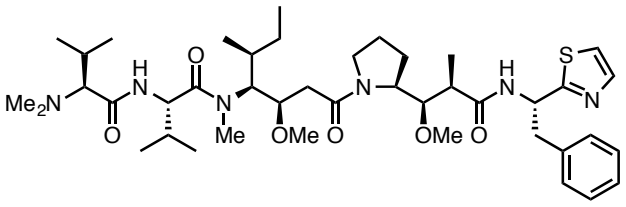


**Fig 6**. Structure of dolastatin 10

In addition, cyclic peptides have higher resistance to endopeptidases and membrane permeability than linear peptides, and are often stably present *in vivo* for a long period of time. Until now, various bioactive cyclic peptides have been reported, such as cyclosporin

(immunosuppressive and anti-inflammatory activity), and many of them have been used as pharmaceuticals[11] (Figure 7).

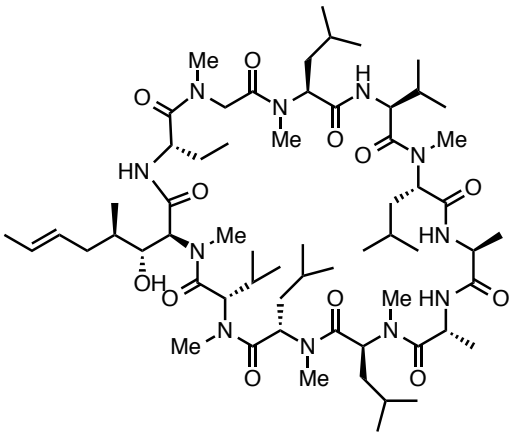


**Fig 7**. Structure of cyclosporin

## 2-4 Inflammation and human biology

Various bioactive cyclic peptides have been reported and many of them are used as pharmaceuticals. Among them, cyclic peptides that have anti-inflammation activity gained our interests. Inflammation is an adaption response of body tissue to harmful stimuli such as chemicals and physical injury. The common signs of inflammation are widely known as heat, pain, redness and so on. Inflammation can be classified as acute inflammation and chronic inflammation. Acute inflammation is formed by the coordinated delivery of blood components (plasma and leukocytes) to the site of infection or injury as the initial response of the body to harmful stimuli[12]. Since acute inflammation is a short-term response, most of them could result in healing. However, chronic inflammation is a prolonged process, in which, inflammatory cytokines, such as TNF-α, IL-6, TGF-β, and IL-10, have been shown to participate in. Chronic inflammation triggers cellular events that lead to a host of diseases, such as hay fever, periodontitis and even cancer. From the above, it is obvious that inflammation is always with us human beings in our daily life.

## 2-5 Cyclic peptide stylissatin A

Stylissatin A (SA, **1**) is a cyclic peptide isolated from the sponge *Stylissa massa*, which was collected on Loroata Island, Papua New Guinea[13] (Figure 8). In general, bioactive cyclic peptides often contain modified amino acids such as *N*-methyl amino acids and D-amino acids, but interestingly, SA is composed of only four kinds of unmodified L-amino acids: isoleucine (Ile), phenylalanine (Phe), proline (Pro), and tyrosine (Tyr). SA is known for its nitric oxide (NO) inhibition function against lipopolysaccharide (LPS) stimulated murine RAW264.7 macrophage cells ($EC_{50}$ = 87 μM). Excessive NO production will result in the formation of peroxynitrites, which causes inflammation and cell damage. Therefore, SA that controls the production of NO, may contribute to the development of new anti-inflammatory agents.

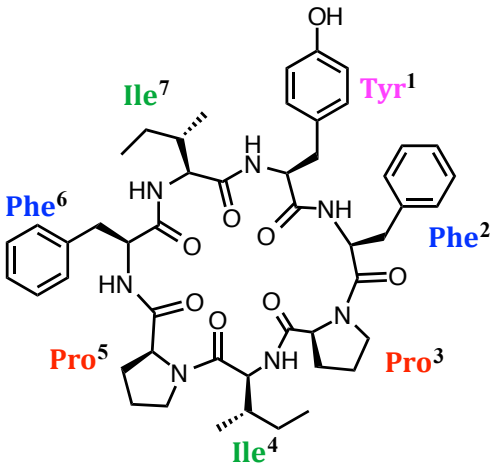


**Figure 8.** Structure of stylissatin A

Due to the uniqueness of its structure, however, it was not known which part in the structure of stylissatin A is important for its biological activity. In addition, the target biomolecules of stylissatin A and their mechanism of action have not been studied so far. Therefore, in order to elucidate the mechanism, structure-activity relationship research of stylissatin A and

identification of target molecule are carried out in this study. What's more, it is also found that SA derivatives not only have anti-inflammation activity but also suppress adipocyte differentiation and fat accumulation during the research. The results of structure-activity relationship research of stylissatin A, identification of target molecule, as well as the new discoveries about adipogenesis inhibition function of SA derivatives will be mentioned in Chapter 5.

# **Chapter 3**. Purpose of this study

This study focuses on the cyclic peptide stylissatin A. Stylissatin A is a cyclic peptide known for its anti-inflammatory activity against macrophages. There are many reports from overseas research groups on the synthesis and biological activity of stylissatin A derivatives[14]. However, the detailed mechanism of this compound has not yet been elucidated. Thus, this study is aimed at identifying the pharmacophore of SA by structure-activity relationship study and clarifying the mechanism of the anti-inflammation activity.

What's more, the author developed several stylissatin A derivatives that have adipogenesis inhibition function against murine fibroblast 3T3-L1 cells in this study. Several cyclic peptides that have either anti-inflammatory effects[15] or fat accumulation inhibitory activity[16] have already been reported. However, to the best of our knowledge, there are no cyclic peptides that show both anti-inflammatory and adipogenesis inhibitory activities with low cytotoxicity. Thus, SA analogs are expected to help understanding new signal transduction systems common to inflammation and adipocyte differentiation, which might contribute to the treatment of diseases as lead compounds. Therefore, the second purpose of this research is to identify the target molecule of SA analogues in 3T3-L1 cells and establish their new mechanism which influences both inflammation response and adipogenesis.

# **Chapter 4**. Material and Method

## 4-1 General

### 4-1-1 Basic

a) All chemicals were obtained commercially unless otherwise noted. Organic solvents and reagents for moisture sensitive reactions were distilled by benzene. All moisture-sensitive reactions were performed under an atmosphere of nitrogen.

b) The reaction was cooled by ice-water bath (0 ℃), ice-NaCl-water bath (–5 ℃), the reaction was heated by oil bath.

c) The reaction solutions were concentrated by rotary evaporator. The freeze drying was performed using vacuum pump lines connected with liquid nitrogen cooled traps.

d) Protein concentration was quantified by Bradford protein assay with Bradford reagents (BIO-RAD, cat. 500-0006) or BCA protein assay with TAKARA BCA Protein Assay Kit (cat. T9300A).

### 4-1-2 Chromatography

a) Fuji Silysia silica gel BW-820MH and Nacalai tesque ODS silica gel COSMOSIL 75$C_{18}$-OPN were used for column chromatography. The column carrier amount and developing solvent was recorded as: [TLC Carrier g (developing solvent)]

b) High-performance liquid chromatography

① Analytical RP-HPLC system using an analytical column [Develosil ODS-HG-5 (Φ 4.6 x 250 mm), Nomura Chemical Co., Aichi, Japan] with eluent pump [PU-2085, JASCO corporation], photodiode array detector [MD-2018, JASCO corporation] and column oven [CO-2060, JASCO

corporation].

② Preparative RP-HPLC was performed on a JASCO PU-2089 plus using a preparative column [Develosil ODS-HG-5 (Φ 20 x 250 mm)] with eluent pump [PU-2089, JASCO corporation], UV/Vis detector [UV-4075, JASCO corporation].

③ The separate condition was recorded as: [column, developing solvent, flow rate (mL/min), detection wavelength]

4-1-3 Solvents and reactants

a) Anhydrous $CH_2Cl_2$, tetrahydrofuran (THF), and *N*,*N*-dimethylformamide (DMF) were obtained commercially from FUJIFILM Wako Pure Chemical Corporation.

b) Preparation of reactants

Triethylamine and diisopropylethylamine:

A commercially available product was heated and refluxed together with calcium hydride in a nitrogen atmosphere for 3 hours or more, and then distilled under normal pressure and used.

c) Preparation of reagents and buffers

1) Protected amino acids (*N*-Fmoc amino acids) were obtained commercially from Watanabe Chemical Industries.

2) PBS (–) pH 7.4 (1x) (cat. 10010-023) were obtained commercially from Life Technologies.

3) PBS-T

10x PBS 100 mL, Tween-20 1mL diluted to 1 L with distilled water.

4) Lysis buffer

50 mM Tris·HCl [pH 7.4] (dissolve Tris 124.1 mg in distilled water adjust the pH to 7.4 by

adding HCl, finally diluted to 20 mL with distilled water) 1 mL, 0.75 M NaCl 1 mL, Triton X-100 50 μL, 100x protease inhibitor cocktail (Nacalai tesque cat. 04080-24) 50 μL, diluted to 5 mL with distilled water.

## 4-2 Experimental operations

### 4-2-1 Cell culture and reagents

Murine macrophage RAW264.7 cells were obtained from American Type Culture Collection (ATCC TIB-71). Murine preadipocyte 3T3-L1 cells were deposited from JCRB cell bank (cell No. IFO50416). Cells were maintained in Dulbecco's modified Eagle medium (DMEM) supplemented with fetal bovine serum (FBS, 10%) in a humidified atmosphere with 5% $CO_2$ at 37℃. Lipopolysaccharide (LPS) was from Santa Cruz Biotech. IL-6 and TNF-α ELISA kit was purchased from R&D Systems. iNOS (#13120) antibody was obtained from Cell Signaling Technology. β-actin antibody was purchased from Novus Biologicals (cat. NB100-56874). HRP-conjugated anti-rabbit IgG antibody was obtained from GE healthcare (NA934-100).

### 4-2-2 Solid-phase peptide synthesis

PetiSyzer Shaking System Description (HiPep Laboratories, cat. PSP-5100) and 5 mL LibraTube with filter (HiPep Laboratories, cat. RT5M100) were used for synthesis. In reaction, the speed adjuster was set around 10. The waste liquid was removed using diaphragm pump that connected with LibraTube through waste tube. The basic operation was performed as bellow.

Weigh out appropriate amount of L-proline 2-chlorotrityl resin (Watanabe Chemical Industries, cat. K01268). Transfer the resin into 5 mL LibraTube, swell resin with agitation for 1 h at rt. in anhydrous DMF (15 mL/g of resin). Transfer a few resin beads for Chloranil test to confirm the presence of free secondary amine of proline and remove the solvent.

① Dissolve protected amino acid (*N*-Fmoc-L- or D-amino acids 5 eq.) and condensing agents (HBTU 5 eq., HOBt 5 eq., *i*$Pr_2$NEt 10 eq.) in anhydrous DMF (0.13 M of resin) in a fresh glass bottle, and stand still for 5 min at rt.

② Add the reactant solvent of ① into reaction LibraTube, and agitate for at least 2 h at rt.

Transfer a few resin beads for Kaiser test or Chloranil test to confirm the reaction progress. Remove the reactant solvent with suction after the condensation was completed, and wash the resin with anhydrous DMF (15 mL/g of resin) for 5 x 1 min.

③ Add 20% piperidine/DMF (v/v) (10 mL/g of resin) into reaction LibraTube, and agitate for 10 min at rt, and then remove the solvent. Repeat once again. Transfer a few resin beads for Kaiser test or Chloranil test to confirm the presence of free amine of amino acid. Wash the resin with anhydrous DMF (15 mL/g of resin) for 5 x 1 min.

Repeat the step ①, ②, ③ to attach the remaining amino acid residues. Following the attachment of final amino acid (L/D-Phe$^{6}$), wash the resin sequentially with $CH_2Cl_2$ (15 mL/g of resin) for 5 x 1 min and MeOH (15 mL/g of resin) for 5 x 1 min. After dehydrating the resin using a flow of nitrogen gas, add 2% TFA/ $CH_2Cl_2$ (v/v) (15 mL/g of resin) into resin, and agitate for 5 x 2 min to cleave the linear peptide from resin and collect the reaction solvent into a fresh glass flask. Wash the resin with $H_2O$ (15 mL/g of resin) for 5 x 1 min and $CH_2Cl_2$ (15 mL/g of resin) for 5 x 1 min, combine all of the filtrate with reaction solvent. The crude linear peptide was obtained after reduced pressure concentration and freeze-drying.

4-2-3 Qualitative testing

a) Kaiser test

Transfer a few resin beads to a glass microtube and wash with ethanol. Add one drop of each of reagent 1 (5 g ninhydrin in 100 mL ethanol), reagent 2 (80 g phenol in 20 mL ethanol), reagent 3 (2 mL of 1 mM potassium cyanide (KCN) in 98 mL pyridine). Hit the glass tube in a preheated oven (300 ℃) to confirm results.

The resin beads will give a dark blue color with the presence of primary amines and will give no color with an *N*-terminal protected amino acid. In the case of the secondary amine of *N*-terminal

proline residues, this test will be not applicable, chloranil test will be performed.

b) Chloranil test

Transfer a few resin beads to a glass microtube and wash with ethanol. Add one drop of each of reagent 1 (2% acetaldehyde in DMF), reagent 2 (2% *p*-chloranil in DMF). Hit the glass tube in a preheated oven (300 ℃) to confirm results.

The resin beads will give a dark red color with the presence of secondary amine and will give no color with an *N*-terminal protected amino acid.

4-2-4 Bioassays

a) Griess assay

RAW264.7 cells ($10^6$ cells/mL, 100 μL/well) were seeded in 96-well plates and incubated for 24 h at 37 °C. Samples (final 0.6–200 μM in 1% MeOH) and LPS (final 1 μM) were added at the same time and the cells were incubated for 24 h. Aliquot of culture medium (100 μl) was mixed with an equal volume of Griess reagent (0.5% sulfamide, 0.05% *N*-naphthylethylenediamine hydrochloride in 5% phosphoric acid) and the optical density at 540 nm was measured with an iMark microplate reader (Bio-Rad Inc.). All assays were performed in duplicate to confirm reproducibility.

b) Cell viability

MTT [3-(4,5-dimethylthiazol-2-yl)-2,5-diphenyl tetrazolium bromide] assay was used to evaluate the cell viability. After the aliquot of culture medium was removed for NO production inhibitory assay as mentioned above, 1.4 mg/mL MTT solution in PBS (50 μL) was added to the cells. After 4 h, the culture medium was removed and the formazan product was dissolved in DMSO (150

μL). Optical density at 540 nm was measured similarly as above.

c) Cell lysate preparation

Cells incubated for 4~5 days to approximately 80% confluence in tissue culture flasks (1.5 x $10^6$ cells) were washed with phosphate-buffered saline (PBS), and treated with 0.25% trypsin–EDTA (Nacalai tesque, cat.35554-64). Suspended cells were collected by centrifugation and washed twice with ice-cold PBS. The cells were lysed in 500 μL of lysis buffer (10 mM Tris·HCl [pH 7.4], 0.75 M NaCl, 1% Triton X-100, 1% protease inhibitor cocktail) with a pestle at 4 °C. All of the following experiments that used cell lysate were conducted at 4 °C unless otherwise noted. To remove most of the intrinsic biotin-binding proteins, the suspensions were centrifuged (10 min, 15000 rpm, 4 °C) and treated with NeutrAvidin agarose resin (Thermo Scientific cat. 29202) equilibrated with 0.1% Tween 20 in PBS (PBS-T) with a rotator for 1 h. The supernatants were collected by filtration to give the cell lysate (0.5 mL) with a concentration of 8 mg protein/mL. The protein concentration of the cell lysate was determined by Bradford protein assay or BCA protein assay.

d) Pull down assay (boiling)

PBS-T (240 μL), 1 mM biotin probe DMSO solvent or DMSO (5 μL), PBS-T balanced NeutrAvidin agarose resin (10 μL / 20 μL) (1:1 (v/v) in PBS) were added into 1.5 mL microfuge tubes and rotated at 4 °C for 2 h. After the removal of supernatants, cell lysate (300 μL) was added, and incubated with a rotator for 2 h. The resin was collected by centrifugation, washed with ice-cooled PBS-T (500 μL × 4), and resuspended in 2× SDS-buffer (30 μL) (Sigma-Aldrich, cat. S3401-10VL). The binding proteins were eluted by boiling at 95 °C for 5 min. SDS-PAGE was performed by using a precast 10% polyacrylamide gel (ATTO Co.), and the gels were stained with a Silver Stain Kit, Protein (GE Healthcare). For competitive elution, affinity purified proteins on the NeutrAvidin agarose (30 μL)

with 600 μL cell lysate similarly prepared as above was incubated with 2 mM SA (**1**) or its derivatives **1a**, **2**, and 2a in PBS-T (40 μL) with a rotator at room temperature for 2 h, and the supernatants were collected by filtration. After freeze-drying, samples were resuspended in 2 × SDS-buffer (20 μL) and boiled at 95 °C for 5 min.

e) Gel electrophoresis and staining

① Gel electrophoresis (SDS-PAGE)

Electrophoresis apparatus (ATTO Corporation, WSE-1150 PageRun Ace) was applied for electrophoresis. The electrophoresis was performed in the condition: 10% polyacrylamide gel (ATTO Corporation, E-T10L), 10x Tris/Glycine/SDS Buffer (BIO-RAD, cat.1610732) diluted one-tenth with Milli-Q water, 21 mA/gel, 85 min.

② Silver staining

Silver staining kit, protein (GE Healthcare Life Sciences, cat. 17-1150-01) was used, all of the solutions were freshly made. Gel was first fixed with solution 1 (5 mL acetic acid, methanol 20 mL diluted to 50 mL with distilled water) and shaked at 25 ℃ for 30 min. Then the gel was sensitized with solution 2 (sodium acetate 3.4 g, sodium thiosulphate (5% w/v) 2 mL, methanol 15 mL diluted to 50 mL with distilled water) at 25 ℃ for 30 min. Gel was washed with distilled water 50 mL for 3 x 5 min and then stained with solution 3 (silver nitrate solution (2.5% w/v) 5 mL and formaldehyde (37% w/v) 20 μL diluted to 50 mL with distilled water) at 25 ℃ for 20 min. Gel was washed again with distilled water 50 mL for 2 x 1 min. After washing, gel was developed with solution 4 (sodium carbonate 1.25 g, formaldehyde (37% w/v) 10 μL diluted to 50 mL with distilled water) at 25 ℃ for 5~15 min until bands appeared. Finally, the reaction was stopped with solution 5 (EDTA-Na· 2H2O 0.73 g dissolved to 50 mL with distilled water) at 25 ℃ for 10 min, followed by washing with distilled water 50 mL for 3 x 5 min. The gel image

was taken by printgraph (ATTO, cat. WSE-5200A).

③ Silver staining (for mass spectrometry analysis)

Gel was first fixed with solution 1 (2.5 mL acetic acid, methanol 24 mL diluted to 50 mL with distilled water) at 25 ℃ for 30 min. Gel was washed with distilled water 50 mL for 2 x 30 min. Then the gel was sensitized with solution 2 (sodium thiosulphate (5% w/v) 200 µL diluted to 50 mL with distilled water) at 25 ℃ for 2 min. Gel was washed again with distilled water 50 mL for 2 x 1 min and stained with solution 3 (silver nitrate solution (2.5% w/v) 5 mL diluted to 50 mL with distilled water) at 25 ℃ for 30 min. Gel was washed with distilled water 50 mL for 2 x 1 min and developed with solution 4 (sodium carbonate 1 g, formaldehyde (37% w/v) 5 µL diluted to 50 mL with distilled water) at 25 ℃ for 15 min until bands appeared. Finally, the reaction was stopped with solution 5 (acetic acid 500 µL to 50 mL with distilled water) at 25 ℃ for 15 min, followed by washing with distilled water 50 mL for 3 x 15 min. The gel image was taken by printgraph (ATTO, cat. WSE-5200A).

f) Inhibition of preadipocyte differentiation and triglyceride accumulation

Murine preadipocyte 3T3-L1 cells were seeded at $2 \times 10^5$ cells/mL ($1 \times 10^5$ cells/well) in 24-well plates in DMEM supplemented with FBS (10%) in a humidified atmosphere containing $CO_2$ (5%). When the cells reached 100% confluence, the culture medium was replaced by the same buffer and cultured for 2 more days. For adipocyte induction, the culture medium was exchanged for the adipocyte differentiation medium (cat. No. F-DM-2-L1, ZenBio, NC, USA) (500 µL per well), and samples in DMSO (0.5 µL) were added at the same time, according to the manufacturer's instructions. After 3 days, the culture medium was replaced by the adipocyte maintenance medium (cat. No. F-AM-1-L1, ZenBio, NC, USA) (500 µL per well), and samples in DMSO (0.5 µL) were added. After 2 days, the culture medium was exchanged again for the same adipocyte

maintaining medium containing samples and incubated for an additional 2 days. To observe fat accumulation in cells, the culture medium was carefully removed and the cells were washed twice with PBS (–), fixed with 8% paraformaldehyde in PBS (–) for 30 min, and washed twice with PBS (–). The cells were washed with 60% aq. *i*-PrOH for 1 min, and then incubated in 1.8 mg/mL Oil Red O in 60% aq. *i*-PrOH for 20 min at room temperature. The cells were again washed with 60% aq. *i*-PrOH for 1 min and washed three times with PBS (–). Phase-contrast images of stained cells in PBS (–) were captured using an Olympus FSX-100 inverted microscope. To quantify the accumulated triglycerides, after the removal of PBS (–), the red-colored dye in cells was dissolved in DMSO (150 μL), and the solution was moved to a 96-well plate. Optical density at 540 nm was measured similarly as above.

To observe the effects of samples on differentiated adipocytes, samples in DMSO were added to the mature cells with the adipocyte maintenance medium and incubated for 2+2 days (including an exchange with the medium with samples). Quantification of the accumulated triglycerides in cells was performed as above. For the measurement of cytotoxicity, preadipocyte 3T3-L1 cells ($5 \times 10^4$ cells/mL in 96-well plates, $5 \times 10^3$ cells per well) in the growth medium were treated with compounds for 72 h. Subsequently, 1.4 mg/mL MTT solution in PBS (50 μL) was added and the mixture was incubated for 4 h, the culture medium was removed and the formazan product was dissolved in DMSO (150 μL). Optical density at 540 nm was measured similarly as above. All assays were performed in duplicate to confirm reproducibility.

g) ELISA

RAW264.7 cells ($1 \times 10^6$ cells/mL for IL-6 and $1 \times 10^5$ cells/mL for TNF-α assays, respectively) were seeded on 96-well plates and incubated for 24 h at 37 °C. Samples (final 0.2–6 μM in 1% MeOH) and LPS (50 ng/mL for IL-6 and 500 ng/mL for TNF-α assays, respectively) were added

at the same time, and the cells were incubated for 24 h. Aliquot of the culture medium was used for ELISA assay.

h) Western Blotting

① RAW264.7 cells ($1 \times 10^6$ cells/mL, 2 mL/well) were seeded in a 6-well plate and incubated for 24 h at 37 °C. Samples (final 20–60 μM in 1% MeOH) and LPS (final 1 μM) were added at the same time, and the cells were incubated for 24 h. Cells were lysed in RIPA buffer supplemented with protease inhibitors (100 μL). Protein concentrations were determined by BCA protein assay reagent according to the manufacturer's instructions. Equal amounts of protein (20 μg) were loaded and resolved by SDS–PAGE, then transferred into PVDF membranes. The membrane was blocked with 0.5% skim milk in water for 1 h at room temperature and was treated with anti-iNOS antibody (1:500) in 3% BSA/PBS for 3 h at 25°C. After washing, the membrane was incubated for 2 h at 25°C with HRP-conjugated anti-rabbit IgG antibody in PBS with 2% skimmed milk (1:4000). The HRP-conjugated bands were visualized with an ECL-prime system (GE Heathcare), and detected by LAS-1000 imaging scanner.

② 3T3-L1 cells ($2 \times 10^5$ cells/mL, 2 mL/well) were seeded in a 6-well plate and incubated for 48 h at 37 °C in DMEM medium. Samples (final 20–60 μM in 1% DMSO) and differentiation medium were added at the same time, and the cells were incubated for 48 h. Cells were lysed in RIPA buffer supplemented with protease inhibitors (100 μL). Protein concentrations were determined by BCA protein assay reagent according to the manufacturer's instructions. Equal amounts of protein (20 μg) were loaded and resolved by SDS–PAGE, then transferred into PVDF membranes. The membrane was blocked with 0.5% skim milk in water for 1 h at room temperature and was treated with anti-PPARγ antibody (1:1000) and anti-C/EBPα antibody

(1:1000) in 3% BSA/PBS for 3 h at 25°C. After washing, the membrane was incubated for 2 h at 25°C with HRP-conjugated anti-rabbit IgG antibody in PBS with 2% skimmed milk (1:4000). The HRP-conjugated bands were visualized with an ECL-prime system (GE Heathcare), and detected by LAS-1000 imaging scanner.

4-2-5 Synthesis of stylissatins and their spectroscopic data

Linear heptapeptide **2**

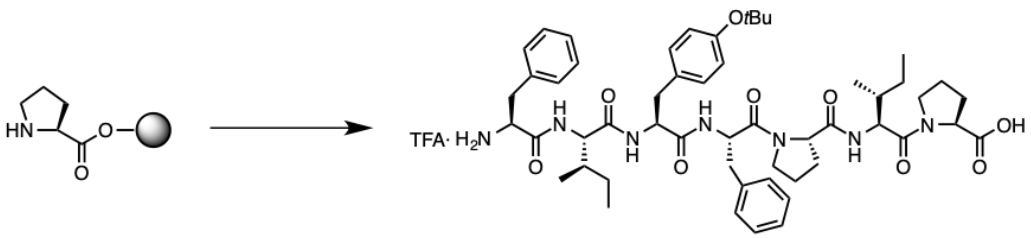


**3** **2**

Linear heptapeptides (**2**) was prepared by solid-phase peptide synthesis using polymer-bound L-proline (Pro[5]) and Fmoc-protected amino acids. 2-chlorotrityl ester polymer-bound L-proline (**3**) (100 mg, 0.60 mmol/g, 60 μmol) was agitated in dry DMF (2 mL) at room temperature for 1 h by a peptide synthesizer PetiSyzer® (HiPep Laboratories, Kyoto, Japan). Following removal of the solvent, a solution of *N*-(9-fluorenylmethoxycarbonyl)- L-isoleucine (106 mg, 0.30 mmol), *N*,*N*,*N*´,*N*´-tetramethyl-*O*-(1*H*-benzotriazol-1-yl)uranium hexafluorophosphate (114 mg, 0.30 mmol), 1-hydroxybenzotriazole (41 mg, 0.30 mmol) and *N*,*N*-diisopropylethylamine (105 μL, 0.60 mmol) in dry DMF (0.5 mL), which had been left to stand for 5 min was added to the resin. The reaction mixture was agitated for 2 h at room temperature. After suction, the resin was washed with dry DMF (1.5 mL, 5 × 1 min). To remove Fmoc groups, 20% piperidine in dry DMF (1.0 mL) was added to the resin, which was then agitated for 10 min followed by suction. This step was repeated followed by washing of the resin with dry DMF (1 mL, 5 × 1 min). The remaining amino acid residues were attached as described above.

Following the attachment of the final amino acid (L-Phe$^{6}$), the resin was sequentially washed with dry $CH_2Cl_2$ (1.5 mL, 5 × 1 min) and MeOH (1.5 mL, 5 × 1 min) and dried with nitrogen gas flow. A solution of 2% aq. TFA (1.5 mL) was added to the resin and agitated for 2 min and filtered. After repeating the cleavage process for four times, the filtrate was combined and concentrated in vacuo. The crude material was partially purified by an ODS column chromatography (COSMOSIL75$C_{18}$OPN 1.5 g, MeOH/$H_2O$ containing 0.1% TFA) to give linear heptapeptide **2** (120 mg, 94%).

Synthesis of cyclic peptide **5** from linear heptapeptide **2**

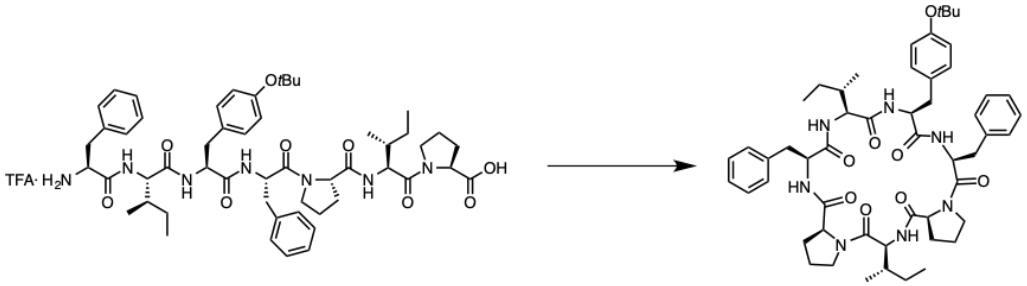


A solution of HOAt (13 mg, 95 μmol) and HATU (36 mg, 94 μmol) and *i*Pr$_2$NEt (16 μL, 95 μmol) in anhydrous DMF (11 mL) was added to linear heptapeptide **2** (20 mg, 19 μmol) at 0 °C under a nitrogen atmosphere. After stirring at room temperature for 48 h, sat. $NH_4Cl$ aq. (10 mL) was added, and the resulting mixture was extracted with EtOAc (3 × 20 mL). The combined organic layer was washed with brine and concentrated. The crude material was purified with an ODS column chromatography (COSMOSIL75$C_{18}$OPN, 1.5 g, MeOH) and reversed-phase HPLC [Develosil ODS-HG-5 (Φ 20 × 250 mm), 88% MeOH, 5 mL/min, 215 nm] to give L-Tyr$^{1}$-*t*BuSA (**5**) (28 mg, 78%) as a white powder.

Stylissatin A (**1**)

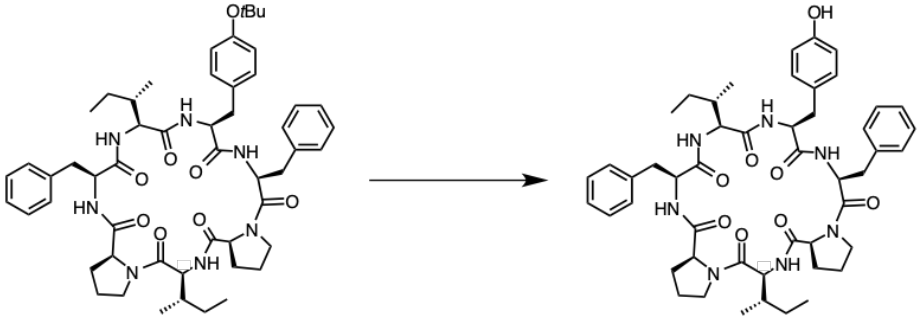


L-Tyr[1]-*t*BuSA (**5**) (7.5 mg, 9.0 μmol) was cooled to –5 °C and TFA/$H_2O$ (95:5, 1.1 mL) was added dropwise. After stirring for 0.5 h, the reaction mixture was stirred for 2.5 h at room temperature. Then the reaction mixture was concentrated, and the crude material was purified by reversed-phase HPLC [Develosil ODS-HG-5 (Φ20 × 250 mm), 85% MeOH, 5 mL/min, 215 nm] to give stylissatin A (**1**) (8.8 mg, quant.) as a white solid.

Linear peptides containing D-amino acids

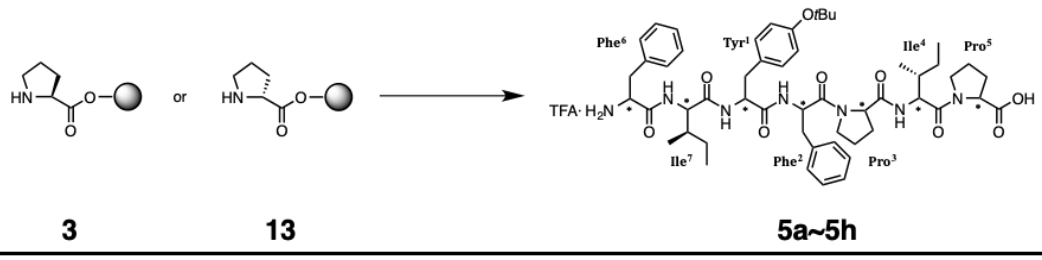


2-chlorotrityl ester polymer-bound L-proline (**3**) or 2-chlorotrityl ester polymer-bound D-proline (**13**) (100 mg, 0.60 mmol/g, 60 μmol) was agitated in dry DMF (2 mL) and synthesized according to the above-mentioned experimental procedure. The crude materials were purified by ODS column chromatography [COSMOSIL75$C_{18}$OPN, MeOH], and cyclization precursors **5a** to **5h** were obtained as white powders (33~99%).

Synthesis of stylissatin A biotin probe (**12**)

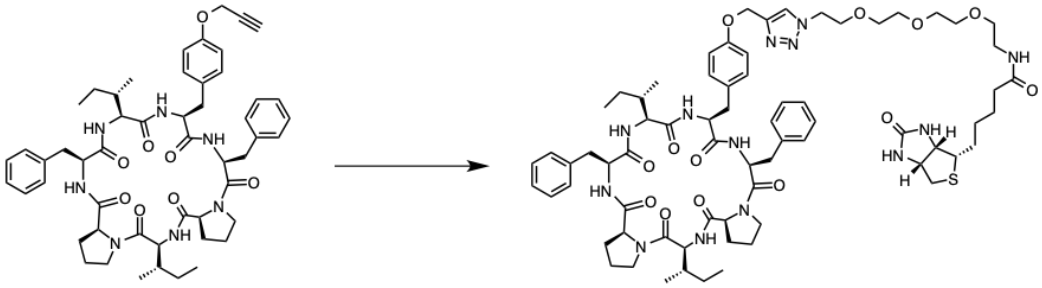

**6** **12**

To a stirred solution of propargyl SA (**6**) (6.0 mg, 7.5 μmol) in *t*BuOH/H2O/THF (1:1:1, 100 μL) were added Biotin-PEG3-azide (Sigma–Aldrich, cat. 762024) (8 mg, 18 μmol), CuSO4 · 5H2O (7 mg, 28 μmol) and 1 M sodium ascorbate aq. (108 μL, 108 μmol). The reaction was stirred at rt for 24 h under a nitrogen atmosphere. After concentration, the crude material was purified with an ODS column chromatography [10 mg, COSMOSIL75C18OPN, Nacalai tesque (50% aq. MeOH)] and reversed-phase HPLC [Develosil ODS HG-5 (Φ 20 × 250 mm), 80% MeOH (0.1% TFA), 5 mL/min, 215 nm] to give SA-BP (**12**) (5 mg, 3.4 μmol, 52%) as a white solid.

# **Chapter 5**. Results and Discussion

## 5-1 Chemical synthesis of stylissatin A

In this study, solid-phase peptide synthesis (SPPS) was used to prepare stylissatin A (SA) and its analogs. SPPS is a useful method to synthesize peptides and proteins. SPPS method has the advantages that the desired linear peptides are generally obtained in high yield and that unnecessary substances and residual reagents are easily removed during the reactions. Thus, speed and simplicity of operation is also a merit of this method[17]. To start SPPS, synthetic route of linear peptide (cyclization precursor of SA) was designed first. Proline residue was chosen as *C*-terminal residue in order to prevent epimerization during cyclization. To reduce steric hindrance during the cyclization, Phe rather than Ile was selected as *N*-terminal, thus, a cyclization site between $Pro^5$-$Phe^6$ was chosen. Thus, cyclization precursor (**2**) was designed (Fig 9).

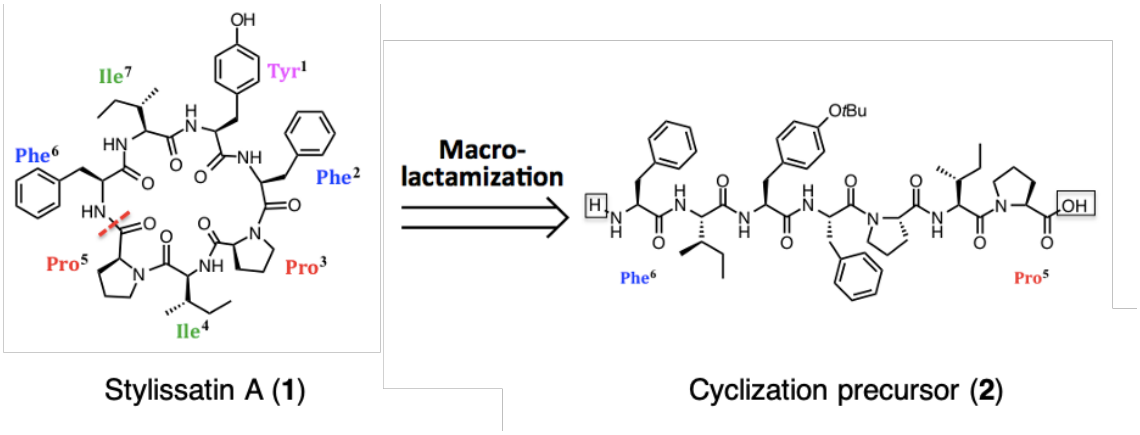


**Fig 9**. Synthetic route for solid-phase peptide synthesis

To get cyclization precursor **2,** synthetic scheme is shown in Scheme 1. The hydroxy group of tyrosine was protected by *t*Bu group to avoid side reactions, but *t*Bu group is easy to be cleaved under strong acidic condition. Thus, L-proline-supported 2-chlorotrityl resin[18] (Barlos resin) (**3**) was used, since linear peptides can be cleaved from the resin under mild acidic conditions. Using

this resin, I planned to synthesize a peptide protected with a *t*Bu group. Heptapeptide **4** was obtained from **3** by repeatedly removing Fmoc group and condensing Fmoc-protected amino acids using HBTU and HOBt, which are peptide coupling reagents to promote dehydration condensation without racemization. Finally, by treating with a 2% TFA in dichloromethane, the linear peptide was cleaved and eluted from the resin to give the cyclization precursor **2** (94% from **3**).

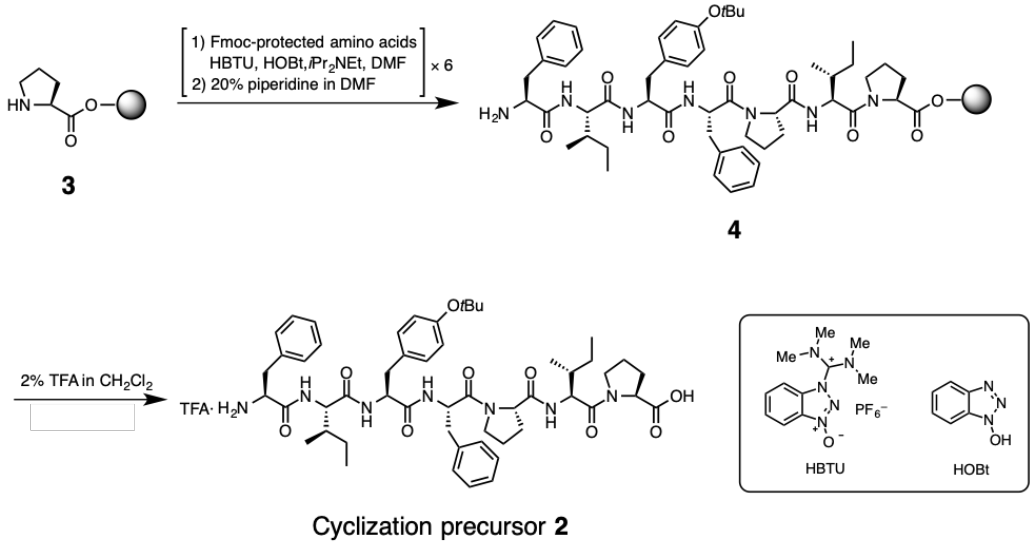


**Scheme 1**. Synthesis of cyclization precursor **2**

After getting cyclization precursor **2**, cyclic peptide (*t*BuSA, **5**) was synthesized (Scheme 2). To avoid epimerization, condensing agents HOAt and HATU were used during cyclization. Compared to HOBt, HOAt has a nitrogen atom on the aromatic ring, and this nitrogen atom has the effect of attracting the amine moieties of the substrate to the reaction site by hydrogen bonding[19]. Therefore, it is particularly effective for cyclization of amines with low nucleophilicity and substrates with large steric hindrance at the reaction site. And HATU is a reagent that produces HOAt in the reaction system and has been reported to be highly effective in suppressing the progress of racemization[20]. As a result, **5** was obtained as a single stereoisomer in good yield

(78%). Finally, removal of the *t*Bu group from **5** with TFA to achieved SA (**1**) (quant.). NMR data of the synthetic SA (**1**) showed good agreement with the natural **1**, confirming that the desired compound was obtained.

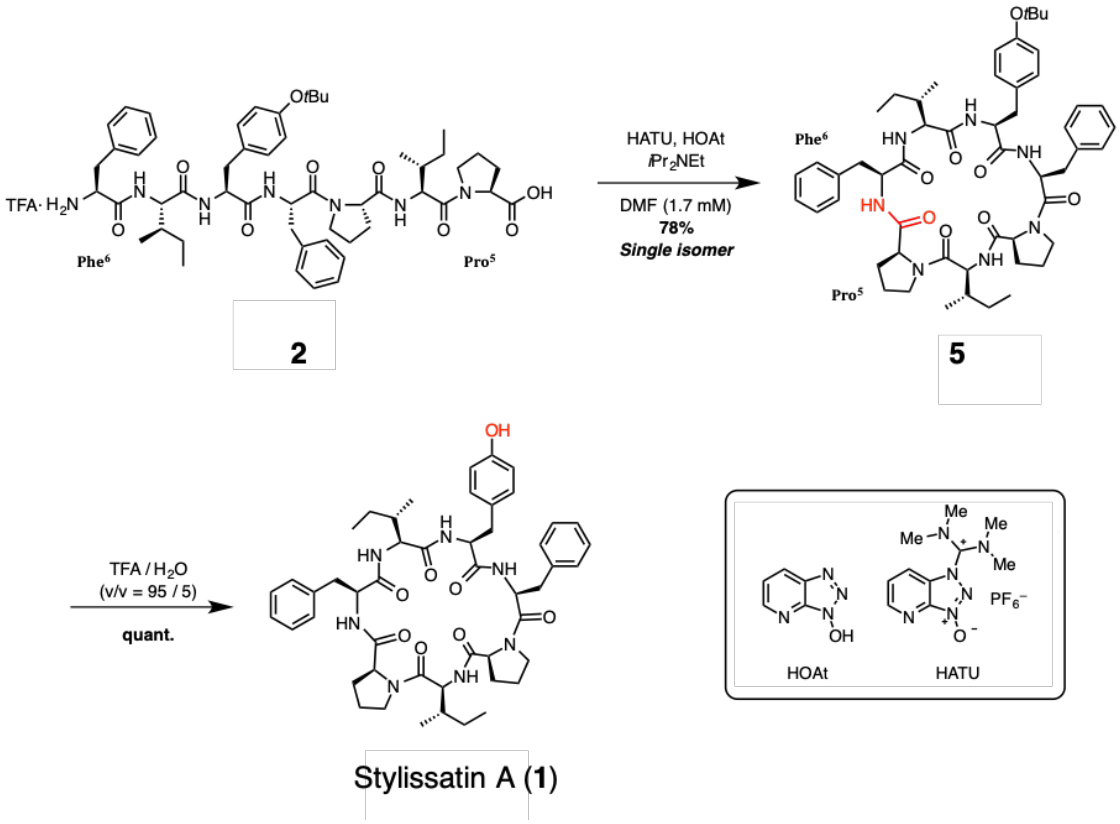


**Scheme 2**. Synthesis of stylissatin A (**1**)

## 5-2 Structure-activity relationship study of stylissatin A – Anti-inflammation activity

Recently, structure-activity relationship (SAR) study has been actively carried out for the creation of excellent drug candidates in drug discovery. Structure-activity relationship study is to investigate which sites of compounds are important for the activity by modifying chemical structures such as substituent groups, conformations, and so on. SAR study is a useful tool to clarify how structures and physicochemical properties (electronic effect, hydrophilicity / hydrophobicity, stereoelectronic effect, etc.) are responsible for the strength of biological activity. Identifying the pharmacophores leads to the elucidation of the mechanism of action of bioactive substances. Therefore, by conducting SAR studies, important findings can be obtained in the design and creation of new pharmaceutical lead compounds[21].

In this research, two approaches for SAR study was investigated (Scheme 3). The first approach is modification of tyrosine residue (**5-11**). Since SA has few functional groups with hydrogen bonds at side chains, the bioactivity was expected to be highly affected by modifying the phenolic

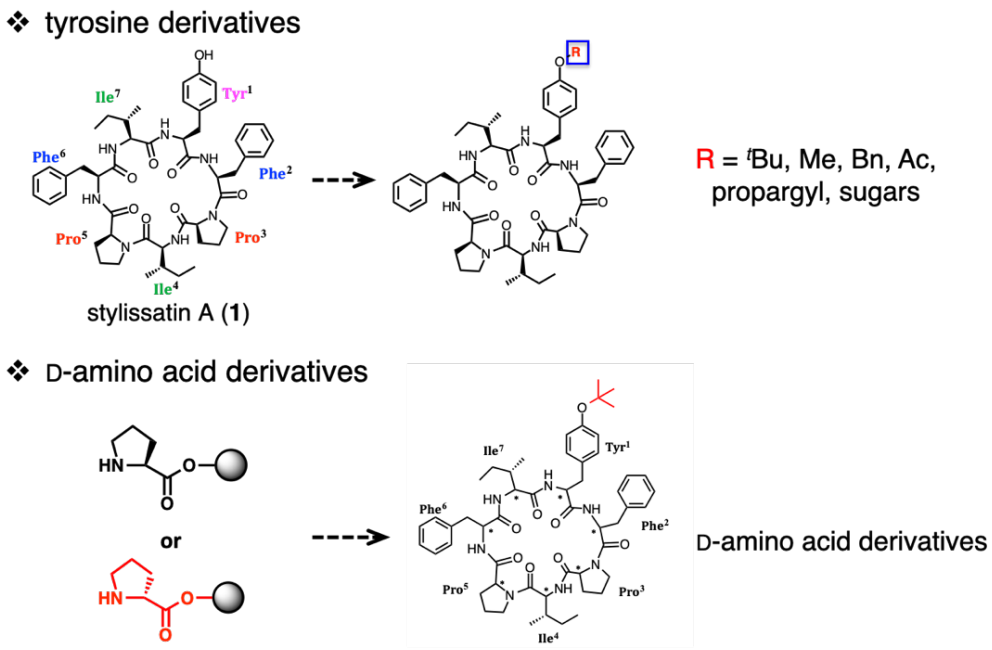


**Scheme 3**. Two approaches for SAR studies

hydroxy group of tyrosine residue. Thus, several typical functional groups such as methyl, acetyl and benzyl groups were chosen to modify OH group. The second one is the introduction of D-amino acids to *t*BuSA (**5**). Introduction of one or several D-amino acids was expected to significantly change the conformation of the macrocyclic peptide skeleton, which may bind more strongly and specifically to the target biomolecules to improve activity.

Table 1 summarize the NO production inhibitory activity (anti-inflammatory activity) and cytotoxicity of SA tyrosine derivatives (**6**-**11**) against LPS-stimulated RAW264.7 cells. The values of the 50% effective concentrations of NO production inhibitory activity and 50% inhibition concentration of cell viability were calculated, and the $IC_{50}$ values of cytotoxicity divided by the $EC_{50}$ values of NO production inhibitory activity were shown as selectivity indexes. Since an ideal anti-inflammatory compound has weak cytotoxicity with potent NO production inhibitory activity, the larger selectivity index value is preferred. As shown in Table 1, all derivatives with ether functional groups, including *t*Bu- (**5**), propargyl- (**6**), methyl- (**7**), and benzyl-group (**8**), showed potent NO production inhibitory activity ($EC_{50}$ 13~17 μM), which were more potent than SA. However, the $IC_{50}$ values of these compounds were decreased which caused

**Table 1**. Anti-inflammatory activity of tyrosine derivatives

| Compound | **R** | NO inhibition[1)] $EC_{50}$ (μM) | Cytotoxicity[1)] $IC_{50}$ (μM) | Selectivity index $IC_{50}$ / $EC_{50}$ |
|---|---|---|---|---|
| SA (**1**) | H | 73 | > 200 | > 2.7 |
| *t*BuSA (**5**) | *t*Bu | 13 | 15 | 1.2 |
| **6** | Propargyl | 16 | 30 | 1.9 |
| **7** | Me | 17 | 30 | 1.8 |
| **8** | Bn | 14 | 18 | 1.2 |
| **9** | Ac | 190 | > 200 | > 1.1 |
| **10** | *O*-Bn glucosyl | > 200 | > 200 | NA |
| **11** | Glucosyl | > 200 | > 200 | NA |

1) Average of two reproducible runs.

the decrease of selectivity. In addition, acetate **9** and glucose derivatives **10** and **11** did not show anti-inflammatory activity even at 200 μM. From this, it was suggested that the NO production inhibitory activity was improved by modifying the tyrosine phenolic hydroxy group with etheric functional groups. The reason why compounds **9**, **10** and **11** did not show significant improvements in activity may be due to their instability for hydrolysis *in vivo*, weak interaction with target molecules, or low cell membrane permeability.

Next, the same evaluation was carried out for SA D-amino acid derivatives, which contain one or two D-amino acids, including D-Tyr[1], D-Phe[2], D-Pro[3], D-*allo*-Ile[4], D-Pro[5], D-Phe[6], D-*allo*-Ile[7], and D-Pro[3,5] analogs (**5a**–**5h**) (Table 2). Comparing to compound **5**, $EC_{50}$ values of **5a**-**5d** and **5f**-**5h** were almost the same, while that of **5e** was approximately 4 times more potent. What's more, **5a**, **5d**, **5g** and **5h** were less cytotoxic and thus the selectivity was improved compared with **5**. In particular, the value of selectivity index of **5a** was the largest, which means compound **5a** showed the most desirable anti-inflammatory activity among all of the synthetic SA derivatives.

**Table 2**. Anti-inflammatory activity of D-amino acid derivatives

| Compound | D-amino acid | NO inhibition[1)] $EC_{50}$ (μM) | Cytotoxicity[1)] $IC_{50}$ (μM) | Selectivity index $IC_{50}$ / $EC_{50}$ |
|---|---|---|---|---|
| SA (**1**) | – | 73 | > 200 | > 2.7 |
| *t*BuSA (**5**) | – | 13 | 15 | 1.2 |
| **5a** | Tyr[1] | 12 | > 200 | > 16.7 |
| **5b** | Phe[2] | 11 | 11 | 1.0 |
| **5c** | Pro[3] | 15 | 16 | 1.1 |
| **5d** | *allo*-Ile[4] | 13 | > 200 | > 15.4 |
| **5e** | Pro[5] | 3 | 15 | 5.0 |
| **5f** | Phe[6] | 19 | 60 | 3.2 |
| **5g** | *allo*-Ile[7] | 20 | 180 | 9.0 |
| **5h** | Pro[3], Pro[5] | 17 | > 200 | > 11.8 |

1) Average of two reproducible runs.

5-3 Effect of D-Tyr[1]-*t*BuSA (**5a**) on the iNOS expression in LPS-treated RAW264.7 cells

iNOS (inducible nitric oxide synthase) is an enzyme induced by LPS to generate nitric oxide (NO) during the inflammation response. Since D-Tyr[1]-*t*BuSA (**5a**) was found to inhibit NO production, it was thought that iNOS expression might be also suppressed by D-Tyr[1]-*t*BuSA (**5a**). Therefore, the expression level of iNOS was examined by Western blot analysis. The result revealed that **5a** significantly inhibited iNOS expression at 20 μM on the LPS-stimulated RAW264.7 cells (Fig 10). One of the pathways that are known to influence iNOS gene expression and subsequent NO release within macrophages is the mitogen-activated protein kinase (MAPK) pathway. Tumor necrosis factor alpha (TNF-α) activates the MAPK pathway, which proceeds to activate nuclear factor kappa-B (NF-κB), a key proinflammatory transcription factor[22]. Thus, it was suggested that the anti-inflammatory activities of SA and its analogs might be related to the signaling pathway that involves TNF-α and NF-κB.

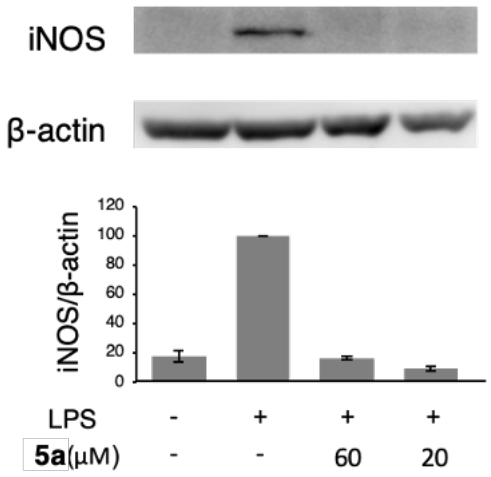


**Fig 10**. Western blot analysis of iNOS and densitometric analysis of the blot. Each bar represents the means and standard deviation (SD) of duplicate determinations.

## 5-4 Quantification of inflammatory cytokines: IL-6 and TNF-α

Based on the Western blot analysis of iNOS, it was suggested that the potent anti-inflammation function of D-Tyr$^1$-*t*BuSA (**5a**) ($EC_{50}$ = 12 μM, $IC_{50}$ > 200 μM) might be related to the signaling pathway that involves TNF-α and NF-κB. In addition, Interleukin-6 (IL-6) is one of the inflammatory cytokines increased by NF-κB activation. Thus, the amounts of TNF-α and IL-6 were quantified by enzyme-linked immunosorbent assay (ELISA). RAW264.7 cells were treated with LPS and **5a** simultaneously, and after 24 h, the amounts of IL-6 and TNF-α in the culture medium were quantified (IL-6: LPS 50 ng/mL, $10^6$ cells/mL, TNF-α: LPS 500 ng/mL, $10^5$ cells/mL). As a result, addition of lipopolysaccharide (LPS) to RAW264.7 cells increased the concentration of both cytokines IL-6 and TNF-α (Fig 11). Meanwhile, treatment with **5a** for 24 h significantly decreased the concentrations of both IL-6 and TNF-α in a dose-dependent manner ($EC_{50}$ = 1.4 and 5.9 μM, respectively). Since the assay conditions of ELISA and NO assay were different, it is not appropriate to simply compare these $EC_{50}$ values, but it was suggested that anti-inflammation function of D-Tyr$^1$-*t*BuSA (**5a**) was due to the inhibition of IL-6 and TNF-α. Since IL-6 and TNF-α are regulated by NF-κB signaling pathway, it was inferred that anti-inflammation function of **5a** might be due to the inhibition of NF-κB, as described in Chapter 5-8 in detail.

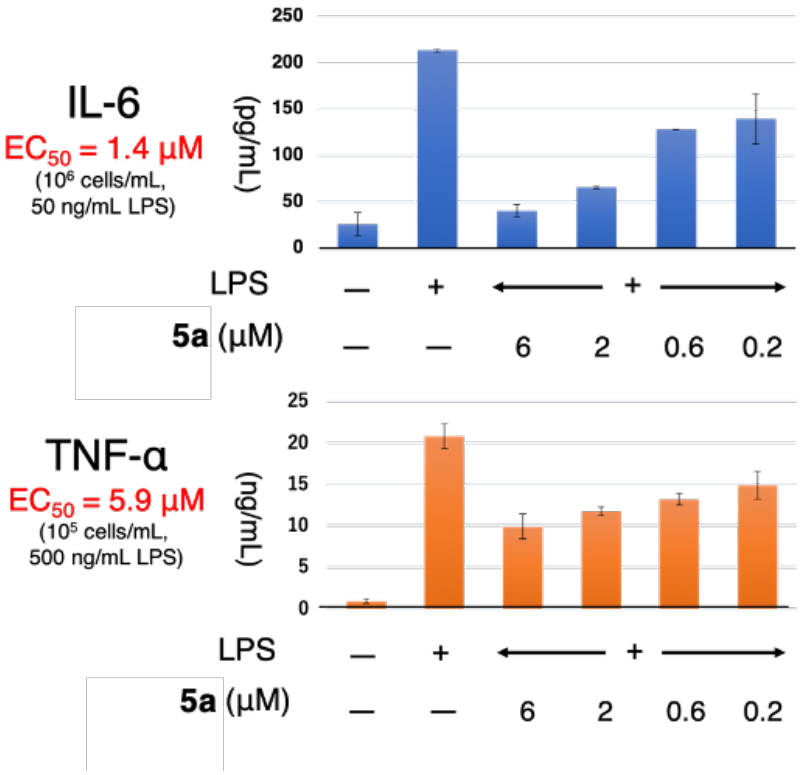


**Fig 11**. Inhibition of IL-6 and TNF-α production by **5a**. RAW264.7 cells were treated with LPS and **5a**. After 24 h, amounts of the inflammatory cytokines on culture medium were quantified by ELISA. Each bar represents the means and standard deviation (SD) of duplicate determinations.

## 5-5 Structure-activity relationship study of SA – Adipogenesis inhibition function

It is known that obesity is a disease closely linked to inflammation. Obesity is not just an increase in body weight and body fat percentage, but also accompanied with the chronic inflammation of adipose tissue, which is closely associated with metabolic disorders such as obesity, insulin resistance, and type 2 diabetes[23]. This "chronic inflammation" is thought to be one of the causes of lifestyle-related diseases such as type 2 diabetes, hypertension and arteriosclerosis. Since SA and its derivatives showed anti-inflammation activity, it was expected that these compounds might also affect adipocyte differentiation. Thus, bioassay was carried out to evaluate the adipogenesis function.

Murine 3T3-L1 fibroblasts have been widely used to investigate the basic cellular mechanisms underlying obesity-related disorders. Murine 3T3-L1 fibroblasts differentiate to mature adipocytes by the treatment with agents such as insulin-like growth factor I. To evaluate the effects of samples on this differentiation process, Oil red O stain was used to visualize triglycerides, which accumulate in adipocytes during cell differentiation. As shown in Figure 12 (a), triglycerides in differentiated cells (right) were visualized by red color, while there are no stained triglycerides in undifferentiated cells (left). To evaluate adipogenesis functions, compounds were added both in adipocytes inducing process and after adipocytes were formed. As shown in Figure 12 (b), fat accumulation of both SA (**1**) and *t*BuSA (**5**) treated cells was reduced compared to that of the differentiated adipocytes treated with only DMSO, which means that both SA (**1**) and *t*BuSA (**5**) potently inhibited the differentiation of murine 3T3-L1 preadipocytes ($EC_{50}$ = 9.1 and 1.9 μM, respectively). To quantify the accumulated triglycerides in cells, the stained triglycerides was dissolved in DMSO and optical density at 540 nm was measured. The values of the 50% effective concentrations of adipogenesis inhibitory activity were

calculated. As a result, $EC_{50}$ values of SA (**1**) and *t*BuSA (**5**) were 9.1 and 1.9 μM respectively. While D-Tyr$^1$-*t*BuSA (**5a**) had the most potent inhibitory effect ($EC_{50}$ = 440 nM). (Figure 13)

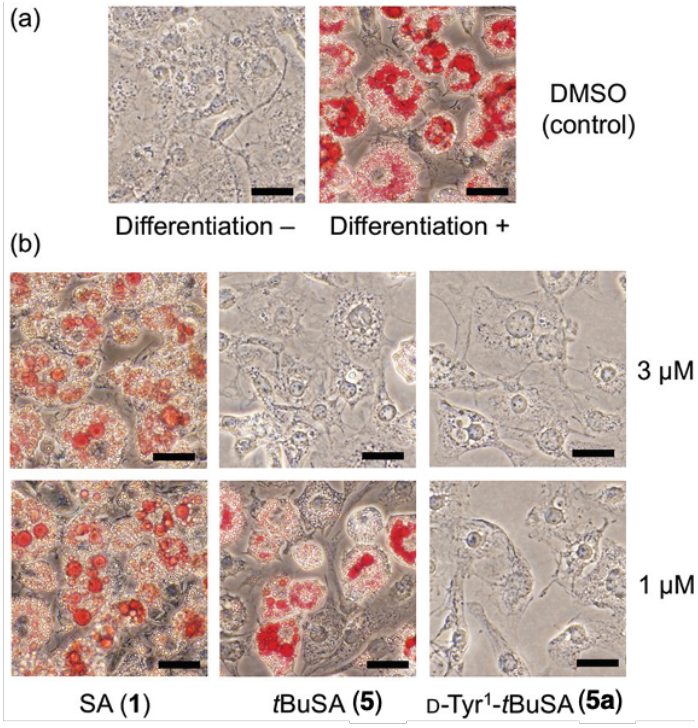


**Fig 12**. Inhibition of adipocyte differentiation on murine fibroblast 3T3-L1 cells by SA analogs. Scale bar = 32 μm. Accumulated triglycerides were visualized with Oil red O stain. (a) Undifferentiated and differentiated cells. (b) Treatment of differentiating preadipocytes with compounds **1**, **5**, and **5a** at 3 μM (top) and 1 μM (bottom) for 7 days.

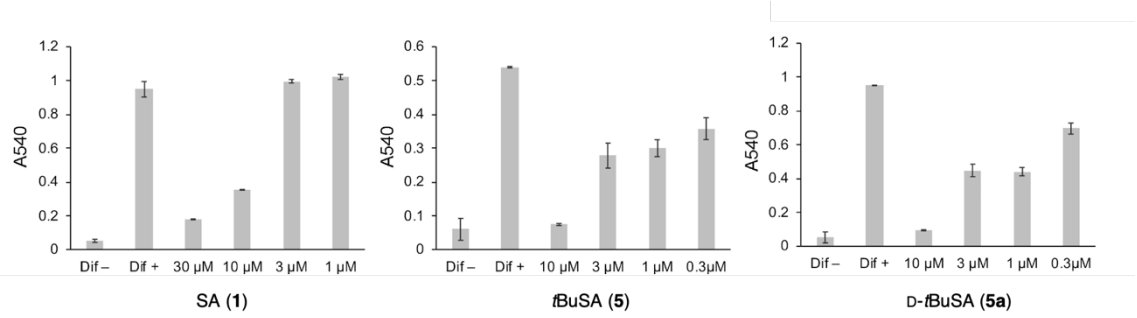


**Figure 13**. Adipocyte differentiation-inhibitory activity of SA (**1**) and its derivatives against murine fibroblast 3T3-L1 cells. Accumulated triglycerides were stained with Oil red O, and the optical density of the dye dissolved in DMSO at 540 nm was measured. Values are the means ± SD of duplicate determinations.

Adipocyte differentiation inhibitory activity of other D-amino acid derivatives (**5b**–**5h**) were also evaluated (Figure 14 and Table 3). Cells treated with **5a**, **5b**, **5e** and **5h** at 10 μM exhibited that most of the fat accumulation was reduced, which suggested that these compounds inhibited the adipocyte differentiation. As a result, **5a** showed most potent adipogenesis inhibitory activity with neglectable cytotoxicity (selectivity index > 450).

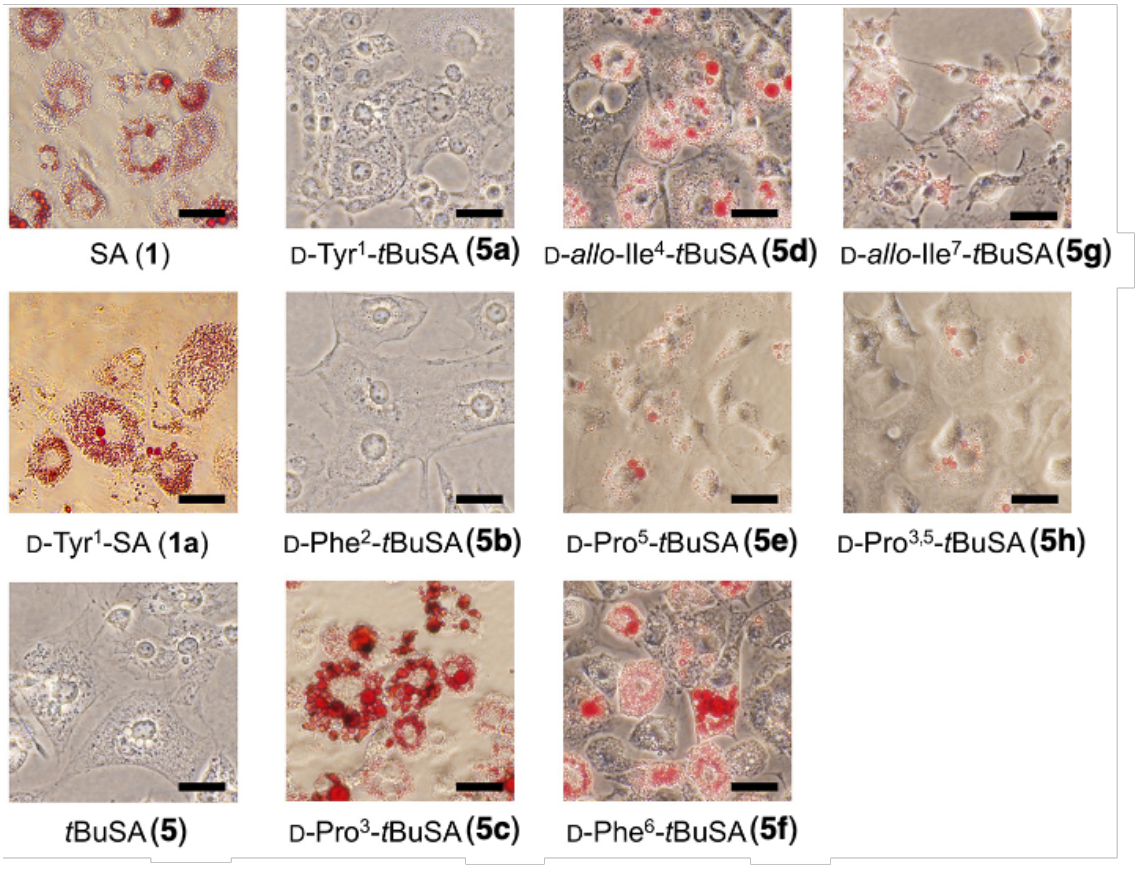


**Fig 14**. Inhibition of the adipocyte differentiation on murine fibroblast 3T3-L1 cells by SA and its analogs at 10 μM. Scale bar, 32 μm. Accumulated triglycerides were visualized with Oil red O stain.

**Table 3**. Adipogenesis inhibition function of D-amino acid derivatives

| Compound | D-amino acid | $EC_{50}$ (μM) | $IC_{50}$ (μM) | Selectivity index $IC_{50}$ / $EC_{50}$ |
|---|---|---|---|---|
| SA (**1**) | – | 9.1 | > 200 | > 22 |
| *t*BuSA (**5**) | – | 1.9 | 21 | 11 |
| **5a** | Tyr[1] | 0.44 | > 200 | > 450 |
| **5b** | Phe[2] | 4.7 | 15 | 3.2 |
| **5c** | Pro[3] | 27 | 11 | 4.1 |
| **5d** | *allo*-Ile[4] | 6.8 | > 200 | > 29 |
| **5e** | Pro[5] | 4.2 | 98 | 23 |
| **5f** | Phe[6] | 4.3 | 190 | 44 |
| **5g** | *allo*-Ile[7] | 5.7 | 170 | 29 |
| **5h** | Pro[3], Pro[5] | 5.0 | > 200 | > 40 |

Average of two reproducible runs.

As in the assay in RAW264.7 macrophages cells described at the Chapter 5-2, selective indexes were increased in an order of **5**, **1** and **5a**, which were same as those for 3T3-L1 cells. These results suggested that there might be a common target for both anti-inflammation and adipogenesis inhibition functions, although the target molecules and mechanism of actions of SA and its derivatives in the RAW264.7 cells and 3T3-L3 cells are still unclear.

## 5-6 Effect of D-Tyr[1]-*t*BuSA (**5a**) on the PPARγ and C/EBPα expression in 3T3-L1 cells

Both PPARγ (Peroxisome Proliferator-Activated Receptor γ) and the C/EBPα (CCAAT-enhancer-binding protein α) are the transcription factors that control adipocyte differentiation. In particular, activation of PPARγ is essential for adipocyte differentiation, as evidenced by the analysis of defective mice[24]. C/EBPα is also considered to play an essential role in maintaining PPARγ expression and insulin sensitivity in 3T3-L1 cells[25]. Thus, PPARγ and C/EBPα protein expression levels of 3T3-L1 cells treated with **5a** in differentiation inducing medium for 48 h were analyzed by Western blotting (Figure 15). First, the protein expression levels of both PPARγ and C/EBPα increased during cell differentiation process. And obviously, **5a** potently suppressed the expression of PPARγ. Especially at the concentrations of 20 and 60 μM, expression levels of PPARγ were fairly lower than that of undifferentiated cells. This might be because **5a** excessively suppressed at the up-stream of PPARγ signaling pathway such as transcriptional regulators C/EBPβ and C/EBPδ, which activate PPARγ expression during the early stage of differentiation in preadipocytes[25]. Thus, by inhibiting these up-stream transcriptional regulators, **5a** suppressed PPARγ expression more effectively than that of undifferentiated cells.

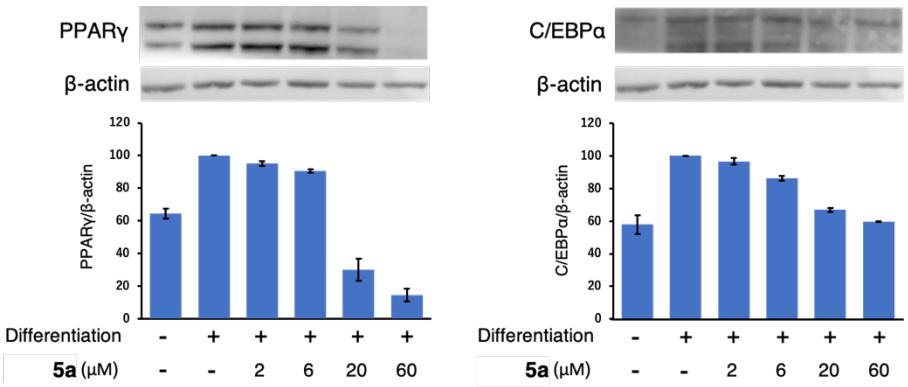


**Fig 15**. Western blot analysis of PPARγ (left) and C/EBPα (right) and densitometric analysis of the blot. 3T3-L1 cells were treated with **5a** in differentiation inducing medium for 48 h. Each bar represents the means and standard deviation (SD) of duplicate determinations.

**5a** also suppresses C/EBPα expression in a concentration-dependent manner, and the expression level was almost same as differentiation(-) at 20 and 60 μM. These results suggested that adipocyte differentiation was suppressed by **5a** through inhibition of PPARγ and C/EBPα protein expression levels.

There have been several reports on PPARγ and C/EBPα antagonists. For example, protopanaxatriol (PPT) is a unique PPARγ and C/EBPα antagonist, which also regulates inflammatory gene expression[26]. Although the real target might be different, if **5a** has similar effect as PPT in vivo, **5a** might be also developed as a lead drug for anti-obesity treatment.

## 5-7 Target identification of SA analogues in macrophage and preadipocyte cells

To elucidate the mechanisms of anti-inflammation and adipogenesis inhibitory activity of SA derivatives, a biotin derivative **12** was synthesized. Huisgen reaction of a propargyl derivative **6** with commercially available biotin-PEG3-azide using copper(I) catalyst gave SA biotin probe **12** in 52% yield (Scheme 4). Biotin probe **12** showed little anti-inflammatory function even at a 200 μM. I assumed that the decrease of NO production inhibitory activity of **12** might be due to the lower cell membrane permeability than SA (**1**) and propargyl SA (**6**). The cell membrane permeability of **12** was significantly changed by the introduction of biotin group and a hydrophilic PEG chain. Still, it was thought that **12** can still bind to the specific target molecules in the cell lysates. Therefore, affinity purification assay was conducted using **12**.

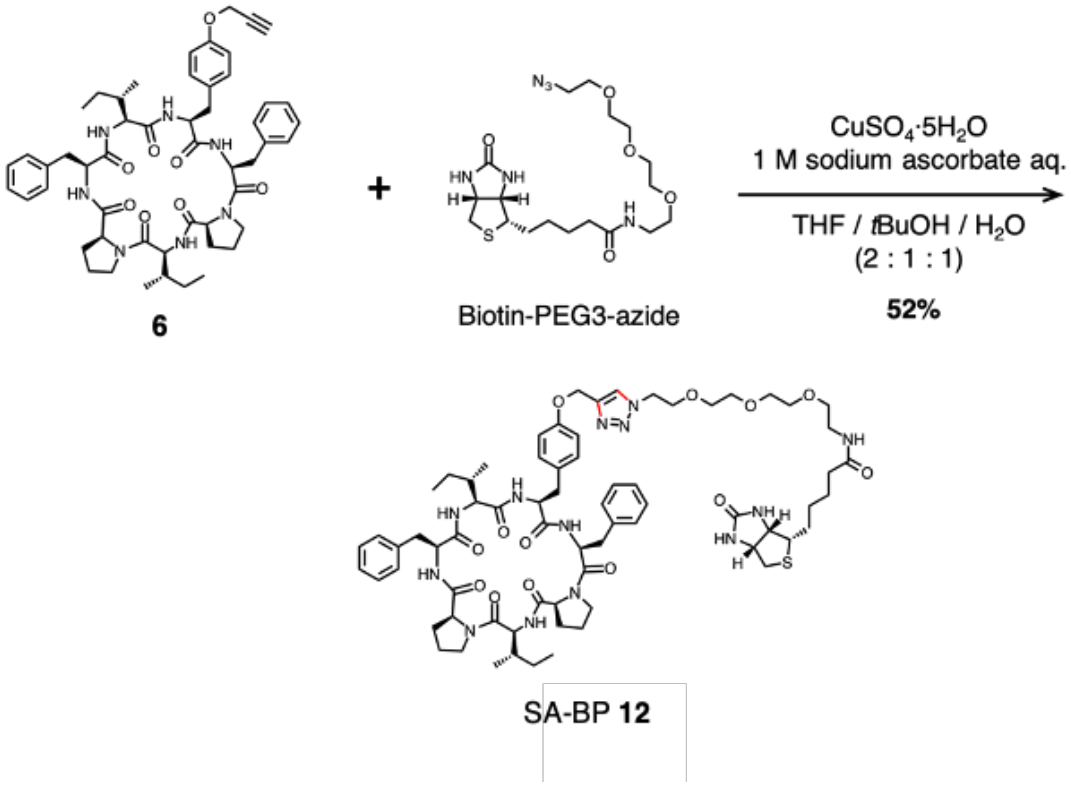


**Scheme 4**. Synthesis of SA biotin probe (SA-BP, **12**)

A typical procedure of pull-down assay using SA biotin probes is illustrated in Figure 17. Firstly, biotin probe is bound to an affinity resin (avidin agarose). Due to the extraordinary high affinity of avidin for biotin group, biotin probes strongly bind to the resin. Then the whole lysate of RAW264.7 cells and 3T3-L1 cells are loaded on the resin, where the target proteins interact with the exposed cyclic peptide moiety. After washing, the target proteins are eluted form the resin by boiling.

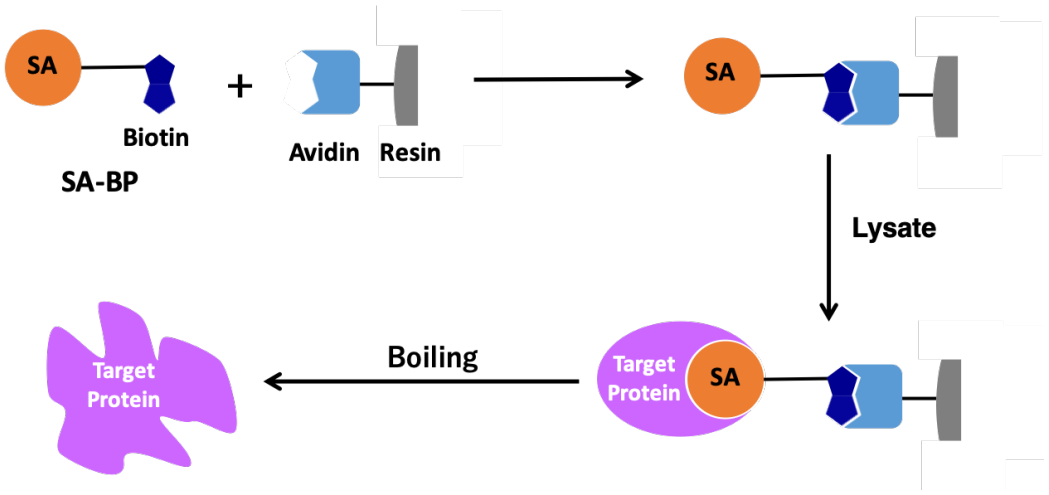


**Fig 17**. Purification of target proteins using affinity resin and SA biotin probe

First, affinity purification of SA target proteins from the RAW264.7 cell lysate was conducted (Figure 18). Boiling elution with SDS buffer resulted in the detection of two specific 45 and 85 kDa proteins. To further evaluate binding specificity, affinity-purified proteins were competitively eluted with SA (**1**) and its three derivatives **1a**, **5** and **5a**. Consequently, only 45 kDa protein was commonly eluted by all four compounds. Peptide mass fingerprinting (PMF) analysis established that this protein was acyl-CoA dehydrogenase, long chain (ACADL). Western blot analysis revealed that the amounts of ACADL competitively eluted by D-Tyr[1] analogs **1a** and **5a** were higher than those of L-Tyr[1] analogs **1** and **5**. These results suggested that D-Tyr[1] analogs might more strongly interact with ACADL than natural SA (**1**). Since the high

anti-inflammatory activity of **5a**, it was assumed that ACADL might be an appropriate target protein.

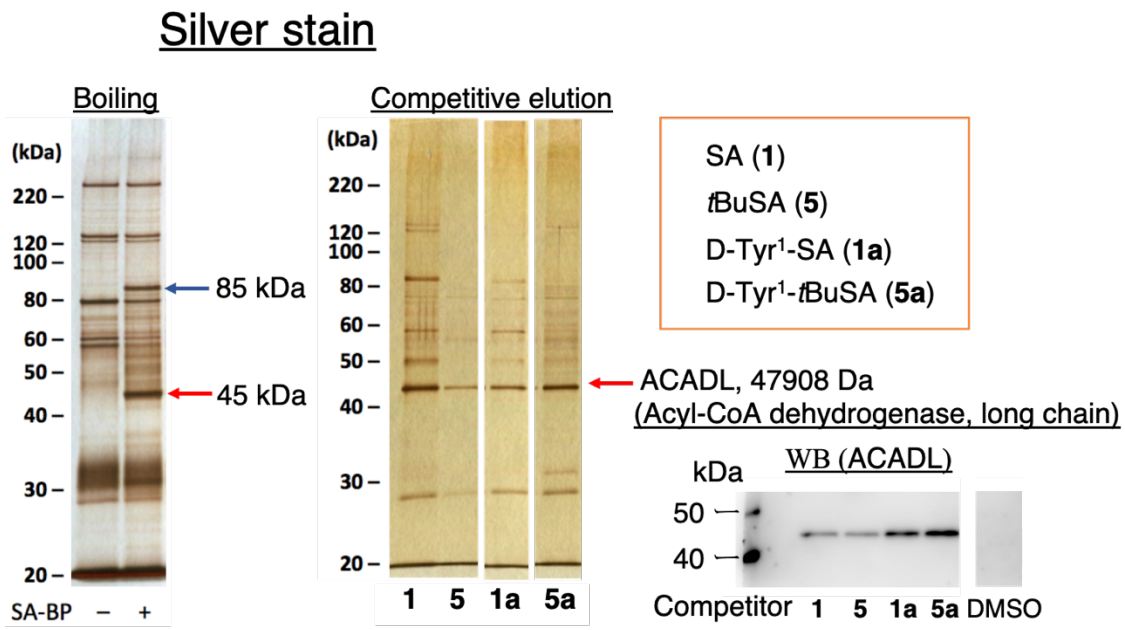


**Fig 18**. Pull-down assay using biotin probes with RAW264.7 cell lysate. Cell lysate was treated with **12** (probe+) or DMSO (probe–). (left) Binding protein (45 kDa) was eluted by the treatment with **1**, **1a**, **5**, and **5a**. (middle) Immunoblotting analysis. (right) Competitively eluted proteins (45 kDa) was detected as ACADL.

In addition, when a pull-down assay was performed using the same biotin probe **12** with cell lysate of 3T3-L1 preadipocytes, boiling elution with SDS buffer resulted in the detection of 45 kDa protein. And WB assay revealed that this 45 kDa protein was also ACADL (Figure 19). Thus, ACADL was the same target proteins of SA (**1**) for both macrophage and preadipocyte cells.

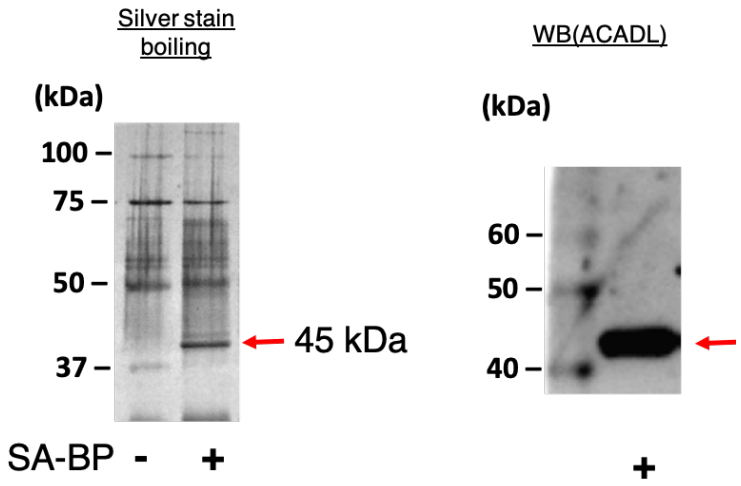


**Fig 19**. Pull-down assay using biotin probes **12** with 3T3-L1 cell lysate. (left) Immunoblotting analysis. (right) Competitively eluted protein (45 kDa) was detected as ACADL.

## 5-8 Assay of acyl-CoA dehydrogenase, long chain (ACADL)

Since ACADL was identified as a common target protein for RAW264.7 and 3T3-L1 cells, an I examine how SA affects ACADL activity. ACADL catalyzes the β-oxidation of long chain acyl-CoA (especially for $C_8$-$C_{18}$ fatty acids)[27], in which acyl-CoA is converted to enoyl-CoA in the presence of flavin adenine dinucleotide (FAD). As shown in Figure 20, when the β-oxidation of acyl-CoA is proceeded, the amount of $FAD^+$ decreases, and when the β-oxidation is inhibited, the amount of $FAD^+$ increases. Thus, FAD levels are often used as a proxy for β-oxidation[28]. Since ACADL activity in cell lysate was unable to be directly evaluated, amounts of FAD was measured as an alternative in this study.

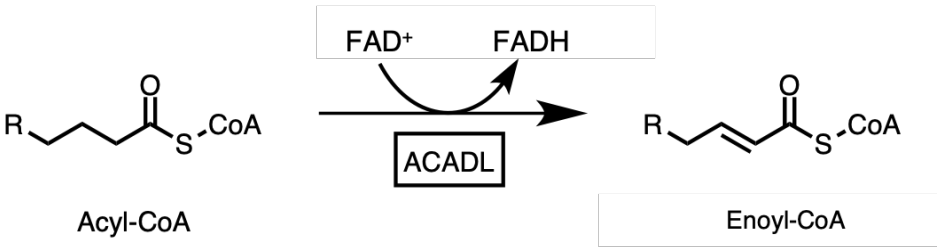


**Fig 20**. Mechanism of β-oxidation by ACADL

The ACADL enzyme activity of the RAW264.7 cells treated with SA (**1**) and D-$Tyr^1$-*t*BuSA (**5a**) were evaluated (Figure 21). Cells were treated with samples for 24 h and the amounts of $FAD^+$ in the cell lysate was quantified. As a result, $FAD^+$ levels were increased to 1.2 and 1.4 times compared to the control by both **1** and **5a** at 60 μM, which means that the β-oxidation level of acyl-CoA was suppressed and the activity of ACADL was inhibited by **1** and **5a**. While this effective concentration was slightly higher than those of the $EC_{50}$ of NO inhibitory activity (ca.10 μM), this might be due to the use of crude cell lysate for ACADL assay. Thus, in the future, purified ACADL solution will be used to improve the specificity of the assay.

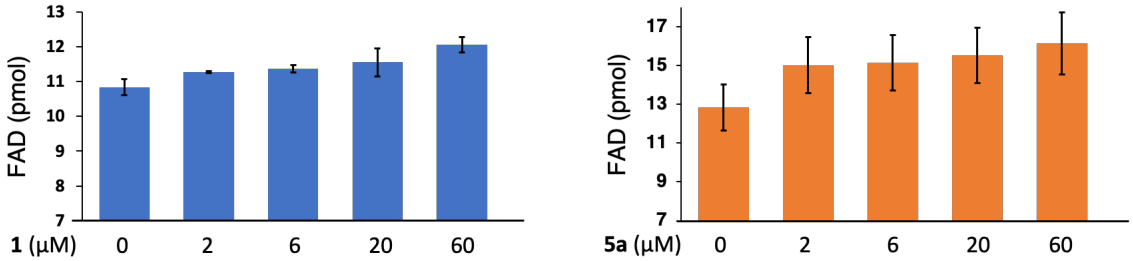


**Fig 21**. Results of ACADL enzyme assay. The amount of FAD in the RAW264.7 cells treated with **1** (left) and **5a** (right) was quantified by FAD kit. LPS was added in all condition.

## 5-9 Proposed mechanism of SA and its derivatives

In this study, ACADL was identified as a common target for anti-inflammatory activity in macrophage cells and adipogenesis inhibition activity in preadipocytes. In addition, enzymatic activity of ACADL was inhibited by SA (**1**) and D-Tyr$^1$-*t*BuSA (**5a**). Herein, the following hypotheses regarding anti-inflammatory and adipogenesis inhibitory functions of stylissatins were considered. ACADL is an enzyme that catalyzes the β-oxidation of long chain fatty acids. For anti-inflammation function, by adding SA analogs, the amounts of liberated fatty acids would increase, which might activate transcription factors PPARα (peroxisome proliferator-activated receptor α) (Figure 22). PPARα activates IκBα by directly binding to the IκBα promoter, which inhibits the function of NF-κB and suppresses the production of IL-6 and TNF-α and the expression level of iNOS, leading to anti-inflammatory activity. Therefore, SA analogs were considered to inhibit ACADL activity. ACADL had not been received much attention so far and could be a new target molecule for anti-inflammatory function. For adipogenesis inhibition function, protein expression level of PPARγ was decreased by **5a** (Figures 15). Inhibited PPARγ generally suppresses adipocyte differentiation and lipid droplet accumulation[29]. Thus, the results that SA derivatives inhibited fat accumulation were reasonable (Figures 12 and 14). Meanwhile, ACADL was also identified as target molecule in 3T3-L1 cells. According to the proposed mechanism in Figure 22, when ACADL was inhibited by SA analogs, increased fatty acids would activate PPARγ. However, this hypothesis did not match to the results of cellular expression levels of PPARγ treated with SA derivatives (see Chapter 5-6). What's more, in the proposed mechanism, activated PPARγ would induce cell differentiation of preadipocytes and result in fat accumulation. However, SA and its derivatives inhibited them and reduced triacylglycerol accumulation levels in mature adipocytes (see Chapter 5-5). Thus, there may be other targets besides ACADL for the adipogenesis inhibition function of SA analogues. These targets have not

been detected by affinity purification because they are trace or unstable in the cell lysate, or they have weak interactions with SA and its derivatives. By improving the structures of chemical probes, such as stereoisomers and the modification of PEG linker moiety, another target molecule for preadipocytes might be found. In order to clarify the real mechanism of stylissatins, in future studies, ACADL will be purified from the mitochondrial fraction of cultured cells or muscle tissues to carry out prompt enzymatic assay. In addition, DNA microarray analysis will also be performed for 3T3-L1 cells to analyze the changes in gene expression levels related to adipocyte differentiation, which might more clearly explain the effects of compounds on intracellular signal transduction on adipogenesis.

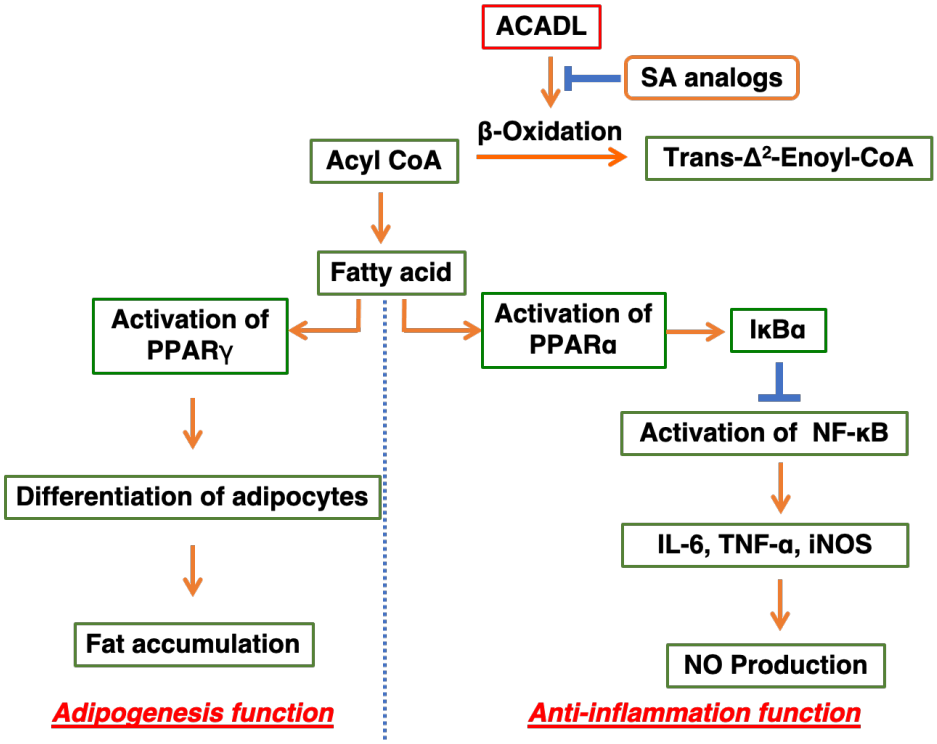


Fig 22. Proposed mechanism

# **Chapter 6**. Conclusion

In this work, experiments were performed to identify the pharmacophore of stylissatin A (SA, **1**) by structure-activity relationship study and clarifying the mechanism of the anti-inflammation activity.

In Chapter 5, SA was synthesized in a high yield. Based on the finding that *t*BuSA (**5**), a synthetic intermediate of SA, showed about 6 times more potent NO production inhibitory activity than SA, structure-activity relationship studies were conducted. It was found that D-Tyr$^{1}$-*t*BuSA (**5a**) showed most potent activity among 16 SA derivatives in both anti-inflammation and adipogenesis inhibition functions with little cytotoxicity. For the anti-inflammation function, ELISA assay proved that anti-inflammation activity of **5a** was due to the inhibition of productions of inflammatory cytokines IL-6 and TNF-α. Western blot analysis revealed that **5a** inhibited iNOS expression, which might directly reduce NO production. Through the pull-down experiments using biotinylated SA derivatives, acyl-CoA dehydrogenase, long chain (ACADL) was identified as the target protein of SA for RAW264.7 cells. And by enzymatic assay of ACADL, compounds **1** and **5a** were found to inhibit ACADL activity. ACADL catalyzes the β-oxidation of long-chain fatty acids. Thus, inhibited ACADL leads to the accumulation of fatty acids, which activate peroxisome proliferator-activated receptors (PPAR). PPARα activators show anti-inflammatory activity through inhibiting of NF-κB activity, which contributes to the inhibition of iNOS expression and also a decrease in NO production. Therefore, it was suggested that the anti-inflammation function of SA analogs was due to the inhibition of ACADL activity.

On the other hand, SA analogs also showed adipogenesis inhibition function. To identify the target molecule of SA analogues in 3T3-L1 cells, the pull-down experiments were carried out. As a result, ACADL was also identified as the target protein for 3T3-L1 cells. And according to the proposed mechanism, PPARγ was thought to be activated by increased fatty acids and result in

fat accumulation, which did not match to the results of cellular expression levels of PPARγ treated with SA derivatives and triacylglycerol accumulation levels in mature adipocytes as described in Chapter 5-5 and 5-6. Thus, for adipogenesis inhibition function of SA analogs, it was considered that there might be other mechanism in 3T3-L1 cells. Further experiments will be performed to elucidate the mechanism of SA and its derivatives. When a new mechanism, which related to both inflammation and obesity, is found in the future, SA analogues are expected to help understanding new signal transduction systems common to inflammation and adipocyte differentiation, which leads to the proposal of new drug discovery targets.

# **Chapter 7**. Abbreviations

aq. = aqueous

COX-2 = cyclooxygenase-2

DMEM = Dulvecco's modified Eagle's medium

DMSO = dimethylsulfoxide

$EC_{50}$ = 50% effective concentration

eq. = equivalent

FBS = fetal bovine serum

HPLC = high performance liquid chromatography

IC50 = 50% inhibitory concentration

IκB = inhibitor κB

IL-6 = interleukin-6

Ile = isoleucine

iNOS = inducible nitric oxide synthase

LPS = lipopolysaccharide

MALDI = matrix-assisted laser desorption / ionization

MS = mass spectroscopy

MTT = 3-(4,5-dimethylthiazol-2-yl)-2,5-diphenyltetrazolium bromide

NF-κB = nuclear factor-κB

NMR = nuclear magnetic resonance

NO = nitric oxide

PAGE = polyacrylamide gel electrophoresis

PBS = phosphate buffered saline

PEG = polyethylene glycol

Phe = phenylalanine

Pro = proline

quant. = quantitative

SDS = sodium dodecyl sulfate

*t*Bu = tertiary butyl

TNF-α = tumor necrosis factor α

Tris = tris(hydroxymethyl)aminomethane

Tyr = tyrosine

v/v = volume per volume

# **Chapter 8**. References


1. Yun B, Yan, Amir R, Hong S, Jin Y, Lee E, Loake G. Plant natural products: history, limitations and the potential of cambial meristematic cells. *Biotech Genet Eng Rev.* **2012**, *28*, 47–60.

2. Caitlin D, Douglas M. Lessons learned from the transformation of natural product discovery to a genome-driven endeavor. *J Ind Microbiol Biotechnol*. **2014**, *41*, 315–331.

3. Gilbert R. Natural Products as a Robust Source of New Drugs and Drug Leads: Past Successes and Present Day Issues. *Am J Cardiol*. **2008**, *11*, 43–49.

4. Cragg G, Newman D. Natural Product Drug Discovery in the Next Millennium. *Pharm Biol*. **2001**, *39*. 8–17.

5. Shen B. A New Golden Age of Natural Products Drug Discovery. *Cell*. **2015**, *163*, 1297–1300.

6. Drew R. A brief history of scuba diving in the United States. *SPUMS Journal*. **1999**, *29*, 173–176.

7. Narahashi T. Tetrodotoxin—A brief history—. *Proc Jpn Acad Ser B.* **2008**, *84*, 147–154.

8. Zheng W, DeMattei J, Wu J, Duan J, Cook L, Oinuma H, Kishi Y. Complete Relative Stereochemistry of Maitotoxin. *J Am Chem Soc*. **1996**, *118*, 7946-7968.

9. Daly J, Lueders J, PadGett W, Shin Y, Gusovsky F. Maitotoxin-elecited calcium influx in cultured cells. *Biochem Pharmacol*. **1995**, *50*, 1187-1197.

10. 砂場大輝. 抗炎症性環状ペプチド stylissatin A の合成構造活性相関および標的分子に関する研究. *筑波大学数理物質科学研究科 修士論文* 2016.

11. Diana F, Karen L. Goa, Paul B, Cyclosporin, *Drugs.* **1993**, *45*, 953–1040.

12. Medzhitov R, Origin and physiological roles of inflammation. *Nature.* **2008**, *454*, 428–435.

13. Kita M, Gise B, Kawamura A, Kigoshi H. Stylissatin A, a cyclic peptide that inhibits nitric oxide production from the marine sponge *Stylissa massa*. *Tetrahedron Lett*. **2013**, *54*, 6826–6828.

14. Farzana S, Almas J, Samreen A, Muhammad N, Shah AZ, Muhammad AZ, Nida D, Ganesan

A. Total synthesis, structural, and biological evaluation of stylissatin A and related analogs. *J Pept Sci*. **2016**, *22*, 607–617.

15. Noh HJ, Hwang D, Lee ES, Hyun JW, Yi PH, Kim GS, Lee SE, Pang C, Park YJ, Chung KH. Anti-inflammatory activity of a new cyclic peptide, citrusin XI, isolated from the fruits of Citrus unshiu. *J Ethnopharmacol*. **2015**, *163*, 106–112.

16. Ito M, Ito J, Kitazawa H, Shimamura K, Fukami T, Tokita S, Shimokawa K, Yamada K, Kanatani A, Uemura D. (–)-Ternatin inhibits adipogenesis and lipid metabolism in 3T3-L1 cells. *Peptides*. **2009**, *30*, 1074–1081.

17. Merrifield R. B. Solid Phase Peptide Synthesis. I. The Synthesis of a Tetrapeptide. *J Am Chem Soc.* **1963**, *85*, 2149–2154.

18. (a) Kleomenis B, Dimitrios G, John K, Giorgos P, Petros S, Yao WQ, Wolfram S. Darstellung geschützter peptid-fragmente unter einsatz substituierter triphenylmethyl-harze. *Tetrahedron Lett.* **1989**, *30*, 3943–3946. (b) Kleomenis B, Dimitrios G, John K, Giorgos P, Petros S, Yao WQ, Wolfram S. Einsatz von 2-chlortritylchlorid zur synthese von Leu$^{15}$ -gastrin I. *Tetrahedron Lett.* **1989**, *30*, 3947–3950.

19. Carpino L.A. 1-Hydroxy-7-azabenzotriazole. An efficient peptide coupling additive. *J. Am. Chem. Soc.* **1993**, *115*, 4397–4398.

20. Valeur E, Bradley M. Amide bond formation: beyond the myth of coupling reagents. *Chem. Soc. Rev.* **2009**, *38*, 606–631.

21. Ravi C, Michael M, Wayne W. Antibody–drug conjugates: An emerging concept in cancer therapy. *Angew. Chem. Int. Ed.* **2014**, *53*, 3796–3827.

22. Sharp GC, Ma H, Saunders PTK, Norman JE. A computational model of lipopolysaccharide-induced nuclear factor kappa B activation: a key signalling pathway in infection-induced preterm labour. *PLoS ONE*. **2013**, *30*, 70180.

23. Fernández-Real J, Pickup J. Innate immunity, insulin resistance and type 2 diabetes.

*Diabetologia*. **2012**, *55*, 273–278.

24. Rasmus S, Ronni N, Susanne M. PPARγ in adipocyte differentiation and metabolism – Novel insights from genome-wide studies. *FEBS Letters*. **2010**, *584*, 3242–3249.

25. Lefterova M, Zhang Y, Steger D, Schupp M, Schug J, Cristancho A, Feng D, Zhuo D, Stoeckert C, Liu S, Lazar M. PPARγ and C/EBP factors orchestrate adipocyte biology via adjacent binding on a genome-wide scale. *Genes Dev*. **2008**, *22*, 2941–2952.

26. Zhang Y, Yu L, Cai W, Fan S, Feng L, Ji G, Huang C. Protopanaxatriol, a novel PPARγ antagonist from Panax ginseng, alleviates steatosis in mice. *Sci. Rep*. **2014**, *4*, 1–12.

27. Indo Y, Teresa Y, Glassberg R, Tanaka K. Molecular cloning and nucleotide sequence of cDNAs encoding human long-chain acyl-CoA dehydrogenase and assignment of the location of its gene (ACADL) to chromosome 2. *Genomics*. **1993**, *11*, 609–620.

28. Bullock H, Shen HF, Boynton T, Shimkets L. Fatty acid oxidation is required for *Myxococcus xanthus* development. *J Bacteriology*. **2018**, *200*, 00572-17. [DOI: 10.1128/JB.00572-17]

29. Chawla A, Schwarz E J, Dimaculangan D D, Lazar M A. Peroxisome proliferator-activated receptor (PPAR) gamma: adipose-predominant expression and induction early in adipocyte differentiation. *Endocrinology*. **1994**, *135*, 798–800.

# **Chapter 9**. Acknowledgement

First of all, my deepest gratitude goes to Professor Masaki Kita, my supervisor, for his constant encouragement and guidance. Without his consistent and illuminating instruction, this thesis could not have reached its present form.

Second, I want to thank Professor Hideo Kigoshi and Professor Shibuya Akira, my supervisors, for their meticulous cares when I was in Nagoya and after I come back to Tsukuba.

Also, I would like to express my heartful gratitude to Professor Takahiro Shibata, Professor Hiroko Isoda, Associate Professor Masahito Yoshida, Dr. Kazunori Sasaki and Dr. Takayuki Oyoshi, who has continuously instructed and helped me a lot.

And I'm deeply grateful to my current and past associates:

in Kigoshi Lab, University of Tsukuba

| | | |
|---|---|---|
| Dr. Atsushi Kawamura | Mr. Taiki Sunaba | Mr. Kota Yamagishi |
| Mr. Shun Watanabe | Ms. Ayaka Taniguti | Ms. Yaping Hu |
| Mr. Masami Okamura | Mr. Yu Seguchi | Mr. Ichimura Fumitaka |
| Mr. Rei Watanabe | Mr. Hikaru Tano | Ms. Mayu Namiki |
| Ms. Momoko Takahashi | Mr. Hiroki Nakane | Mr. Kei Akemoto |
| Mr. Keita Iio | Mr. Yuto Tamazaki | Mr. Keisuke Mitsugi |
| Ms. Yuri Inami | Mr. Yiwen Zhao | Mr. Jun Tsuzaki |
| Mt. Shoma Tojo | Mr. Ryuya Higuma | Mr. Koji Yamaguti |
| Mr. Takuma Ishihara | Mr. Tetsuya Inaba | Ms. Imari Kikuchi |
| Mr. Tomonari Nogichi | Mr. Kohei Hano | Mr. Shu Hosono |
| Mr. Shota Konisi | Mr. Tomonari Jo | Mr. Mituki Hagimoto |

in Kita Lab, Nagoya University

| | | |
|---|---|---|
| Dr. Maho Morita | Mr. Atsushi Arai | Mr. Junya Ikuma |
| Ms. Akari Fujieda | Ms. Yiting Sun | Ms. Minako Hirukawa |
| Mr. Didik Huswo Utomo | Mr. Kohei Obata | Ms. Toshiko Takenaka |

Finally, I would like to express my gratitude to my beloved family for their moral support and warm encouragement in me all through these years.